

CHARACTERIZATION OF
FLASH-ELICITED VOLTAGE TRANSIENTS
IN CHLOROPLAST-LIPID BILAYERS

Thesis for the Degree of M. S.
MICHIGAN STATE UNIVERSITY
THEODORE EDWARD MILLER, JR.
1973



ABSTRACT

CHARACTERIZATION OF FLASH-ELICITED VOLTAGE TRANSIENTS IN CHLOROPLAST-LIPID BILAYERS

BY

Theodore Edward Miller, Jr.

Bilayer lipid membranes (BLM) are formed from extracts of spinach chloroplast. Electrical transients are seen to originate across the BLM in response to microsecond flash excitation under a variety of asymmetrical conditions. Flash excitation clearly delineates at least two voltage generative processes often of opposite polarity that under continuous illumination give rise to only a single steady-state voltage value. Thus a mechanistic description accounting for the steady-state value alone may not be sufficiently comprehensive. The "spike" feature of the continuous illumination dependent voltage time course can be predicted from the flash experiments. A chemical gradient of FeCl_3 gives rise to a rapid microsecond voltage transient with polarity, action spectrum, and risetime that suggest that photo-electrons from excited chlorophyll reduce Fe^{+3} . However in most cases, there exists also a slow electrical transient responding to applied electrical field or pH gradient. The slow component peaks at typically 200 ms, depending upon the RC time of the BLM system, and fits the following description:
$$V(t) = V_o \left[1 - \exp \left(-\frac{t}{RC} \right) \right] \exp (-\lambda t).$$
 Specific agents such as ascorbic acid and p-benzoquinone quench completely the slow photosensitive

Theodore Edward Miller, Jr.

process (voltage or pH gradient-induced) leaving the fast (FeCl_3 chemical gradient-induced) photoeffect unmodified; others such as iron and bromide similarly enhance selectively the slow response. Clearly, the steady state membrane potential under continuous illumination depends upon whether such quenching or enhancing agents are present. To the extent that this system retains the machinery requisite for elements of the primary event of photosynthesis, it is useful to have such controls for purposes of identifying excited states operative in photosynthesis.

CHARACTERIZATION OF FLASH-ELICITED VOLTAGE
TRANSIENTS IN CHLOROPLAST-LIPID BILAYERS

By

Theodore Edward Miller, Jr.

A THESIS

Submitted to
Michigan State University
in partial fulfillment of the requirements
for the degree of

MASTER OF SCIENCE

Department of Biophysics

1973

ACKNOWLEDGMENTS

I wish to extend my sincerest appreciation to those who inspired and encouraged this study, especially research advisor Dr. H. Ti Tien.

I also gratefully acknowledge support from the National Institutes of Health Training Grant No. GM-01422 of Michigan State University and the College of Osteopathic Medicine of Michigan State University.

TABLE OF CONTENTS

	Page
ACKNOWLEDGMENTS	iii
LIST OF TABLES	v
LIST OF FIGURES	vi
Chapter	
I. INTRODUCTION	1
II. LITERATURE REVIEW	6
III. EXPERIMENTAL	14
Apparatus	14
Extraction Techniques	18
Procedure	19
IV. RESULTS	22
Introduction	22
The Fast Component	23
The Slow Component	26
Lambda Decay	27
The Quenching Phenomenon	34
V. DISCUSSION	47
VI. ADDITIONAL RESULTS	69
Dual Component Voltage Decay	69
Chl-BLM Mechano-Electric Oscillation	72
Photo-EMF Internal Resistance	73
VII. SUMMARY	83
BIBLIOGRAPHY	85

LIST OF TABLES

Table	Page
1. List of equipment	21

LIST OF FIGURES

Figure	Page
1. Chl-BLM flash illumination apparatus with delay system for resolving microsecond transients	16
2. Flash response in the presence of 10^{-2} M FeCl_3 in the inner chamber compared to the dark chl-BLM RC transient	24
3. Biphasic response in the presence of FeCl_3 and negative applied voltage	28
4. Top trace: Slow Component in the presence of applied voltage only. Bottom trace: enhanced photovoltage transient subsequent to the addition of 0.023 M NaBr	30
5. Chl-BLM Slow Component decay kinetic compared to membrane RC transient	32
6. Top trace: immediate elimination of the Slow Component upon addition of 10^{-3} M ascorbate. Bottom trace: gradual disappearance of the slow transient in the presence of 10^{-4} M ascorbate	35
7. Top traces: biphasic responses in the absence of quencher. Bottom traces: reduced Slow Component in the presence of 2×10^{-3} M NaN_3 , 2×10^{-3} M ascorbate	37
8. Quencher elimination of a bromide-enhanced slow response	39
9. Slow transient quenching by 10^{-3} M tannic acid while 10^{-3} M FeCl_3 -induced Fast Component remains unmodified	41
10. Quenching by 10^{-3} M ascorbate in the presence of repeated flash illumination (~ 50 Hz)	43
11. Light and dark current-voltage relationship of chl-BLM prior and subsequent to the addition of 10^{-3} M ascorbate	45

Figure	Page
12. RC system analogous to chl-BLM and voltage waveform for switch closed 1 ms	49
13. Experimental Slow Component decay and plot of log V values versus time	53
14. Experimental chl-BLM slow response waveform and points predicted from given approximation.	56
15. Slow Component waveforms and points calculated using $R_m C_m$ and λ data included in figure	59
16. Additional Slow Component waveforms and points calculated from $R_m C_m$ and λ data included in figure.	61
17. Slow Component peak time dependence upon effective R_m	63
18. Transient BLM photoconductivity dependence upon quencher concentration	66
19. Logarithmic plots of chl-BLM voltage decays for potentials applied 0, 6 and 20 seconds	70
20. Open circuit BLM potential oscillation synchronous with mechanical vibrations.	74
21. Effect of low external shunt resistance on the FeCl_3 -induced Fast Component	77
22. Arrangement used to measure photocurrent output of chl-BLM	79
23. Membrane photovoltages returned to zero by application of external voltage biases.	81

CHAPTER I

INTRODUCTION

All biological machinery requires fuel in the form of energy-rich chemical bonds such as the anhydride pyrophosphate bond of the nucleotide adenosine triphosphate (ATP). In aerobic organisms chemical free energy is made available in this form as reduced foodstuffs are oxidized by highly efficient mechanisms to CO_2 . The major energy packaging process, oxidative phosphorylation, occurs as electrons are passed along the respiratory electron transport chain to oxygen within the membranous cristae of mitochondria; electron transfer through this redox system can be monitored with sensitive differential cytochrome adsorption spectroscopy techniques. Thus, in this case energy is conserved and transferred in a manner relatively open to study.

However, the primary photosynthetic electron transfer reaction, which ultimately provides the energy required for the synthesis of these fuel molecules while most commonly oxidizing water to oxygen in green plants, occurs within stacked thylakoid membranes (grana) of chloroplasts and involves membrane-dependent energy transduction. As a consequence of the structural and functional complexity of photosynthetic membranes, the investigator encounters unique obstacles. Biochemical reactions subsequent to formation of the primary reductant and primary oxidant via chlorophyll-sensitized energy transduction

are relatively easily delineated. According to the Z-Scheme (Arnon, 1967; Boardman, 1968) nicotineamide adenine dinucleotide phosphate (NADP^+) is reduced and ADP phosphorylated during non-cyclic photo-phosphorylation. These products are utilized to reduce CO_2 to hexoses and other carbohydrates via the Calvin Cycle (Bassham, 1957). However, the precise in vivo mechanism of chlorophyll-sensitized primary reductant and oxidant formation is as yet obscured by the following features:

i) Regardless of the electron donor and acceptor, in all photo-synthetic organisms light energy enables electrons to flow from electron donor to electron acceptor against the normal gradient of standard reduction potentials. Light energy, therefore, causes electrons to flow in reverse toward an energy-rich state as opposed to their flow in respiration. The chloroplast's system for constraining this to occur rather than simple energy degradation is of a unique design not readily amenable to analysis.

ii) Photoexcitation of pigment molecules is very rapid, requiring less than 10^{-15} seconds, and singlet excited molecules possess mean lifetimes of approximately 10^{-5} to 10^{-9} seconds (Moore, 1963); consequently, rapid detection instrumentation is necessary.

iii) The grana, flattened vesicles or thylakoids stacked transversely across the chloroplast, contain essentially all the chloroplast's photosynthetic pigments and the enzymes necessary for the primary light-driven reactions (Lehninger, 1970). The fundamental importance of the thylakoid membrane is implicit. Thus an investigation of chlorophyll photochemistry in solution is not necessarily a study of the role of chlorophyll in photosynthesis. A membranous matrix for

the chlorophyll would render the system more highly representative of the in vivo arrangement.

Mueller, Rudin, Tien, and Wescott prepared the original artificial bimolecular lipid membranes (BLM) (Mueller, Rudin, Tien, and Wescott, 1962), the first successful attempt since the postulation of the lamellar bilayer structure for the plasma membrane (Gorter and Grendel, 1925). The bimolecular nature of BLM has been demonstrated (Goldup, 1970; Tien, 1971); amphipathic constituents are oriented such that aliphatic chains are immersed in the hydrophobic lipid interior of the BLM while charged and polar regions extend into the surrounding aqueous medium. Electron microscopy, x-ray diffraction and birefringence as well as circular dichroism studies corroborate that the photosynthetic apparatus consists of such a highly ordered lamellar array (Menke, 1967; Branton, 1969; Mühlethaler, 1966).

Tien recently undertook to investigate whether a BLM exhibiting energy transducing properties could be constituted from photoactive pigments to facilitate the study of photosynthetic primary processes (Tien, 1968). Indeed, chlorophyll/lipid membranes formed from spinach chloroplast extract exhibited the photovoltaic effect, a direct demonstration of in vitro energy transduction originating from a primitive reconstituted thylakoid membrane.

This work has undertaken to investigate the nature of the photo-flash stimulated voltage transient in chlorophyll bilayer lipid membranes under application of chemical and electrical gradients. By permitting voltage generative kinetics to be clearly delineated, micro-second flash illumination offers the optimum method for identifying reaction orders and lifetimes.

There are two basic photoresponse initial phase kinetics, viz. a microsecond time duration chemically induced response and a slower pH or voltage gradient-induced transient peaking typically at 200 ms after illumination. In particular this work has provided identification of the kinetics of the mechanism responsible for the slow response (component C) of the chl-BLM to flash illumination. Since previous kinetic models for the slow transient (Tien and Huebner, 1973) were unable to describe precisely the slow response waveform, they were thought to be at best marginally adequate. The following kinetic description, however, fits the data quite satisfactorily. Specifically this model is original in two major respects:

I. The decay process had been assumed to be first order RC; we now understand that it is first order with rate constant $\lambda < (RC)^{-1}$ and any process slower than $(RC)^{-1}$ across the membrane network is kinetically independent of RC. This possibility was originally not considered. Also the initial phase kinetics of the slow response are now seen to be first order with $(RC)^{-1}$ as rate constant; prior opinion was that some rate constant unrelated to dark membrane electrical characteristics was appropriate. Thus the slow transient is described by a unique mathematical expression that assumes a time constant identical with dark membrane first order RC and a first order exponential decay independent of RC, i.e.,

$$V(t) = V_o [1 - \exp(-Kt)] \exp(-\lambda t)$$

where $K = (RC)^{-1}$ and λ is a first order rate constant. The fit to experimental waveforms is excellent. This expression, then, yields novel information concerning BLM photoproperties; that is, two diametrically dissimilar mechanisms are operative: the current-generating fast effect

driven by chemical reduction potential gradients and the slow effect due to somewhat enhanced membrane conductivity.

II. Secondly, recent evidence indicates that we may begin to assign chlorophyll triplet character specifically to the slow phenomenon. Since conductivity returns slowly to equilibrium in a first order manner, responsible metastable state lifetimes are easily calculated. In addition, without modifying the microsecond transient, heavy atoms known to enhance singlet* \longrightarrow triplet* intersystem crossing (McGlynn, 1969) selectively augment the slow response magnitude while other in vitro chlorophyll triplet quenchers (Livingston, 1960; Fujimori, 1957; Livingston, 1963) eliminate only the slow transient. Together with calculated lifetimes this provides compelling evidence of the molecular nature of the slow response.

CHAPTER II

LITERATURE REVIEW

In the brief space of time since the original reports of photoelectric effects from BLM (Tien, 1968), several other investigators recognizing invariable association of in vivo light absorbing pigments with membranes have also initiated studies of the BLM photoeffect. Currently, perhaps ten laboratories world-wide are examining the photoexcitability of appropriately modified artificial bilayers. However, the researcher who gleans BLM photoeffect data and postulated mechanisms from the accumulated literature in this infant science anticipating that such a study will lead to a comprehensive, thorough understanding of bilayer photosensitivity is mistaken. This circumstance is due to the fact that the artificial bilayer photosystems under investigation from laboratory to laboratory are vastly different; i.e., membrane and bathing media compositions vary, modifiers used to confer excitability differ, and the photovoltage detection systems are of assorted designs and capabilities. Nonetheless, as we are acquiring information concerning various aspects of the underlying phenomenon, such variegated independent investigations will ultimately lead to a precise explanation of the BLM light response.

Soon after the appearance of Tien's announcement of light-induced phenomena in chlorophyll BLM in Nature, July 1968 (Tien, 1968), T.R. Hesketh undertook to determine to what extent radiation heating

contributed to the observations although Tien had employed a heat filter. Hesketh reported (Hesketh, 1969) that the waveform of the temperature variation in the membrane aperture volume detected by thermocouple correlated with Tien's voltage transients; he continued to report detection of a "genuine" light effect using an infrared background to insure heat fluctuations of less than 0.1°C . It has since been shown that the open circuit photovoltage amplitude and bias are strictly dependent upon electron acceptor gradients and polarities; also, voltage transient characteristic times are unrelated to membrane and bulk heat capacity values (Tien and Verma, 1970; Huebner and Tien, 1972).

There followed reports of assorted photoeffects in the presence of various modifiers. Mauzerall and Finkelstein pointed out photoconductivity in cholesterol/ α -tocopherol BLM in the presence of polyiodide (Mauzerall and Finkelstein, 1969). They postulated that the polyiodide ion is a photosensitized charge carrier across the membrane. Ullrich and Kuhn using egg lecithin in octane membranes observed photoeffects employing dyes in one aqueous compartment (Ullrich and Kuhn, 1969). They reported a photovoltage action spectrum corresponding to the dye absorption spectrum and suggested that electrons are donated across the bilayer from the oxidized dye. Tien, incorporating visual pigments all-trans-retinal and β -carotene into oxidized cholesterol BLM, measured β -carotene-sensitized photoresponses and photoconductivity effects possibly induced by cis-trans conformation changes subsequent to the absorption of photons (Tien and Kobamoto, 1969). In all of the above investigations it was found that the action spectra for the photoelectric effect compared well with the

absorption spectra of the bilayer or its constituents indicating that interactions between the light and the membrane were responsible for the observed effects.

Several publications next appeared which suggested a growing interest in BLM light phenomena from a purely physical point of view as reports of organic membrane photo energy transduction to electrical and chemical form captured the imagination of physical chemists and solid state physicists alike. Kay and Chan at Philco-Ford Corporation undertook to ascertain whether bona fide charges are induced in the BLM upon irradiation (Kay and Chan, 1969). Using α -tocopherol in decane membranes and UV radiation in the presence of iodide, they concluded on the basis of current-voltage characteristics of the membrane that generated charges were essential as part of the mechanism leading to the photoelectric effect. A similar publication later followed supporting these observations (Kay and Bean, 1970).

Suspecting that since the bilayer forms a distinct phase from the film-forming solution, the chlorophyll to lipid ratio in the membrane may be quite different, Alamuti and Luger further characterized chlorophyll bilayers in terms of pigment concentration and relative amounts of chlorophyll and lecithin, a stabilizing surface active amphipathic phospholipid (Alamuti and Luger, 1970). Dioleoyl lecithin in n-decane membranes with various proportions of chlorophyll a exhibited a fluorescence maximum at a composition indicating a 3:1 phosphatidyl choline to chlorophyll a ratio and $\sim 10^{13}$ chlorophyll a molecules per cm^2 . Trissl and Luger later confirmed Tien's observations of electrical potentials elicited from chlorophyll BLM using redox agents and agreed that a redox process occurs after optical excitation

of pigment molecules in the membrane (Trissl and Läuger, 1970). The physical characterization of photoactive BLM continued as Cherry, Hsu, and Chapman developed a technique for measuring absorption spectra of pigments incorporated into lipid membranes (Cherry, Hsu, and Chapman, 1971). They employed a differential Cary 14 Spectrophotometer absorption cell containing a series of bilayer-supporting apertures to overcome the low optical density afforded by a single thin membrane. However, a more sensitive method was proposed by Van and Tien who observed that the photoelectric effect action spectrum correlated closely with the BLM absorption spectrum (Van and Tien, 1970).

Tien, meanwhile, continued his investigations into various aspects of the bilayer light phenomenon itself. The redox nature of the process was all but confirmed as photoemfs were elicited according to the redox properties of modifiers added to the BLM system (Tien and Verma, 1970). Studies into visual early receptor potentials using retinal bilayers proceeded as Tien and Kobamoto determined that the time course of photopotentials showed a biphasic mode quite similar, under appropriate conditions, to that of early receptor potentials (Kobamoto and Tien, 1971). An extension and refinement of this work appeared later (Kobamoto and Tien, 1972).

A series of papers reported results from a somewhat altered membrane/modifier arrangement. Oxidized cholesterol BLM, inert to visible light due to the lack of pigment among the bilayer constituents, exhibited photosensitivity in the presence of particular aqueous dyes and light sensitive inorganic ions (Verma, 1971; Pant and Rosenberg, 1971). Verma indicated that prior postulated redox mechanisms for pigment-containing BLM (Tien and Verma, 1970) occur also in the

non-pigmented bilayer instance although the response characteristics reflect the altered arrangement of dye, membrane, electron donor, and electron acceptor; and Pant and Rosenberg observed a correlation between the classical Becquerel Effect of excited ion and metallic electrode electron exchange and the BLM light phenomenon, the membrane in its capacity as electronic conductor fulfilling the role of the metallic electrode.

Using a dual beam spectrophotometer and fluorescence photomultiplier arrangement, Luger et al. extended their previous study of lipid bilayer composition (Steinemann, Alamuti, Brodmann, Marschall, and Luger, 1971). A maximum chlorophyll concentration of 3×10^{13} per cm^2 was reaffirmed, at which amount the bilayer absorption spectrum was shifted to longer wavelengths indicating an interaction among porphyrin rings in the film. However, they continued to report that the addition of the oxidizing agent potassium peroxodisulfate to one external aqueous phase "destroyed exactly half of the chlorophyll in the biface", an inference drawn from the observation that fluorescence fell by half upon addition of oxidant. Huebner in a subsequent letter to the editor (Huebner, 1972) pointed out that he had observed enhanced photoeffects from chlorophyll BLM in the presence of peroxodisulfate indicating that fluorescence is quenched by a process which enhances electrical charge transport suggesting that pigment is not destroyed but excitation energy in the presence of oxidant is simply lost to fluorescence and utilized instead in charge transport. Luger et al. later published chlorophyll BLM dichroism data indicative of porphyrin ring orientation in the biface (Steinemann, Stark, and Luger, 1972) and offered in another paper (Trissl and Luger, 1972) a theory of

photoelectric effects in BLM based on two different models, an approach deemed necessary by them earlier when they acknowledged: "Ullrich and Kuhn" noted that "a transient potential spike is observed" under continuous illumination. "In contrast to this," other systems "develop a stationary photovoltage under continuous illumination. This indicates that the mechanism of charge separation is quite different in both systems" (Trissl and Luger, 1970). Indeed, Ullrich and Kuhn later presented further data from egg lecithin in n-octane membranes in the presence of an aqueous cyanine dye and restated the observation that photopotentials are not sustained under continuous illumination but appear rather as spike potentials (Ullrich and Kuhn, 1972). They proceeded to construct an interfacial dipole polarization model highly analogous to the classical polarized electrode problem in electrochemistry in which charge separation at the electrode interface introduces a capacitive element which effectively blocks constant current flow. Perhaps a more useful enterprise would have been to assemble and analyze a membrane photo system capable of sustained charge transport facilitating chemical energy transfer relevant to the *in vivo* modus operandi.

A careful study of chloroplast extract bilayers in the presence of inorganic modifiers and exciting continuous illumination was initiated by Ilani and Berns who asserted on the basis of an equivalent electrical circuit approach that an effective low internal resistance photobattery may be considered introduced upon excitation in response to a redox potential gradient (Ilani and Berns, 1972). Meanwhile, Hong and Mauzerall employed the voltage clamp technique to eliminate current flow to and from the BLM capacitive element in order to isolate

trans-membrane charge flow in response to microsecond flash exposure (Hong and Mauzerall, 1972). They concluded that photoresponses to pulsed light are specific to the thin bimolecular region rather than the thick annular region.

Tien continued his investigation into properties of photoactive BLM as he reported the results of a careful characterization of chlorophyll bilayer photosensitivity and rectification produced by ferric chloride in addition to open circuit voltage, current, and resistance measurements as a function of light intensity (Loxsom and Tien, 1972); Tien also directly addressed the question of whether genuine electronic processes can occur in a bilayer structure immersed in an aqueous environment and concluded that such processes might indeed occur (Tien, 1972). Also, Huebner and Tien presented the results of an analysis of microsecond flash excitation of chlorophyll BLM using an improved low output impedance fast voltage transient detection system (Huebner and Tien, 1972) that revealed the interesting combination of an extremely rapid voltage rise concomitant with a much slower independently induced transient upon flash illumination. This arrangement provided a convenient means for measuring both the large microsecond current necessary to charge the membrane capacitance within the given risetime and simultaneously, the distinct photoconductivity transient which occurs over an extended period; this conductivity alteration merits attention since it represents a slight shorting pathway shunted across the dark conduction paths which serves to additionally diminish the true photoeffect. The entire merit of their approach was that it afforded an elegant means to concurrently measure both true photoemf and conductivity enhancement.

Tien and Huebner subsequently characterized the individual components comprising the photoeffect (Tien and Huebner, 1973) but acknowledged some difficulty in interpreting the slow response, "Component C", as a current generating process with RC decay although the fast response fit this assumption quite well; that is, a satisfactory kinetic description of the slow component was lacking. This thesis addresses itself to resolving this difficulty and further characterizing the effect in terms of recently discovered chemical quenchers and enhancers specific to the slow response in the hope that an accurate kinetic description and modifier sensitivity profile of the response might extend our understanding of its molecular details.

CHAPTER III

EXPERIMENTAL

Apparatus

The characteristic high electrical impedance properties of chlorophyll bimolecular lipid membranes along with their unique optical features and delicate structural nature require that a suitable experimental apparatus be employed; also since upon microsecond flash excitation extremely rapid electrical transients originate across chlorophyll BLM under a variety of asymmetrical conditions, it was necessary to detect their kinetics using special instrumentation.

An excellent site for stable membrane formation was afforded by a millimeter circular aperture in a 10 ml teflon cup. Extremely high teflon resistivity guaranteed negligible shunting currents across the highly resistive membrane and in addition, the teflon cup contributed only about 3 picofarads capacitance, again negligible compared to the typical BLM capacitance of 5000 pf. The teflon cup rested in a glass cell designed to present surfaces normal to both the incident illuminating light beam and the direction of observation, minimizing light scattering and image distortion. Each of the chambers separated by the membrane aperture was provided with a saturated KCl asbestos fiber-junction salt-bridge calomel electrode to maintain electrical continuity from solution to external circuitry. The electrodes were connected to a high input impedance buffer amplifier mounted as close

as possible to the electrodes to minimize input cable length, a precaution necessary because the high impedance BLM circuit is quite sensitive to spurious external signals and, in addition, cable capacitance increases with length, augmenting the amplifier input RC time and thus impairing instrumental response capabilities. A Philbrick FET operational amplifier (model 1021) was employed as an excellent impedance buffer since it features a common mode rejection ratio of 10^{10} and input impedance of 10^{12} ohms. As a result of its stability and low drift characteristics, this amplifier is well suited for unloading the BLM high impedance source and providing rapid signal rise time. The amplifier output was displayed and recorded on a Tektronix dual beam storage oscilloscope screen.

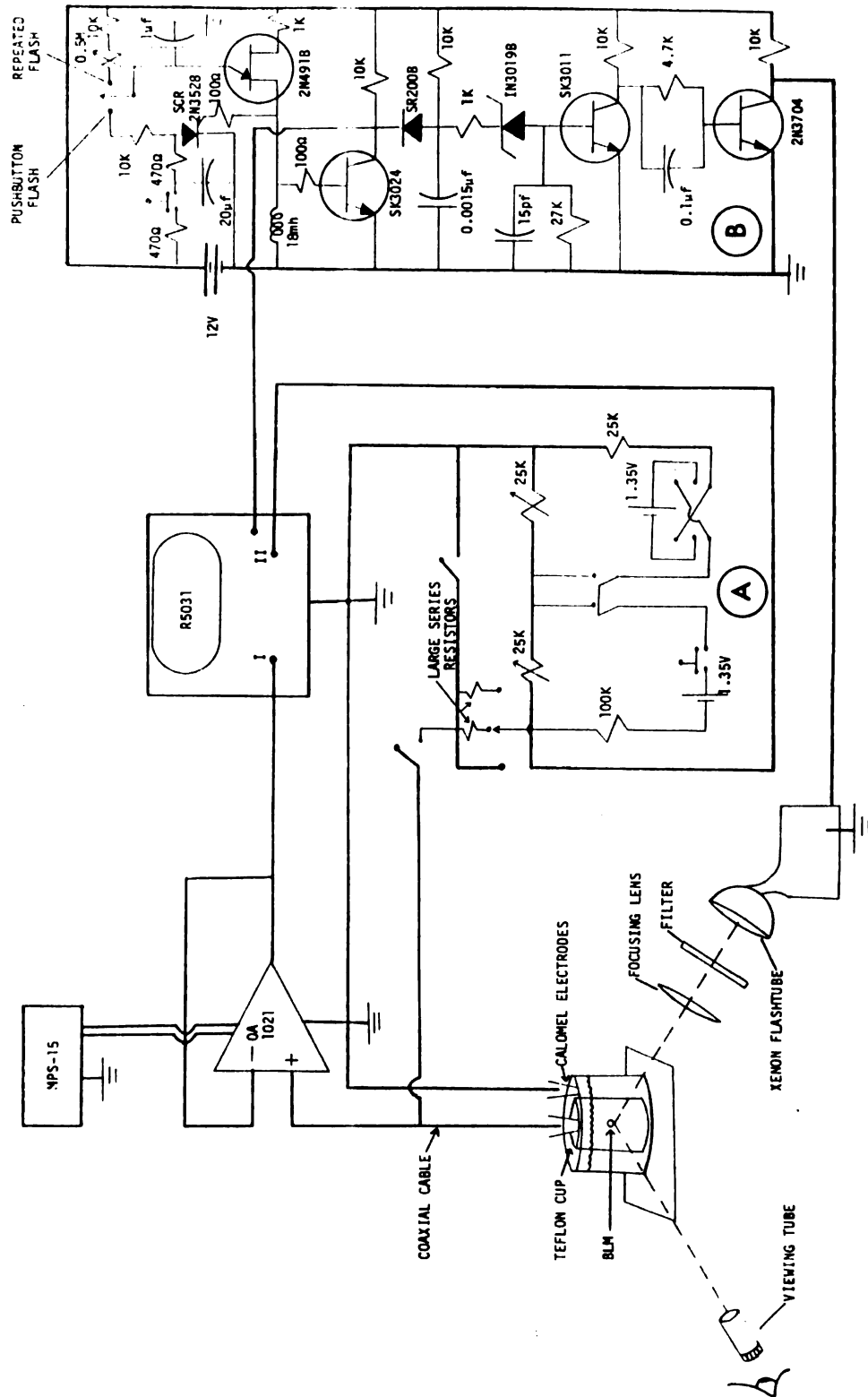
The electrodes were shunted with a variable voltage source also monitored by the oscilloscope and large series resistances for applying trans-membrane potentials and measuring membrane resistance and capacitance. Illumination of the membrane area was furnished by a General Radio Stroboslave xenon flash tube assembly that produced a peak value of 10^9 lux at the membrane with 1/3 peak times separated three microseconds. For resolving microsecond transients, a transistor triggering device synchronized stroboscopic flash and oscilloscope sweep.

To shield the BLM support cell including electrodes and buffer amplifier from undesirable external illumination and electrical noise a large Faraday cage was constructed of a wooden frame, fiberboard, and copper screening grounded to the outer chamber electrode. The entire apparatus is schematically shown in Figure 1.

Figure 1. Chl-BLM flash illumination apparatus with delay system for resolving microsecond transients.

A. Series resistance and variable applied voltage source.

B. Oscilloscope and strobe trigger.



Extraction Techniques

The following procedure was followed in the preparation of chloroplast BLM-forming solutions. Fresh spinach was purchased from a local market and ribs and stalks were removed from a 10-oz. portion. The leaves were washed with distilled water, dried thoroughly, and then added slowly to a Waring blender at low speed with 300 mls of isotonic 0.5 M sucrose plus buffer at pH 7.5. When all the leaves had been added high speed was used for 30 seconds; the homogenized mixture was filtered through 4 to 6 layers of cheesecloth to further remove structural cellulose and isolate chlorophyll-rich chloroplasts. The filtrate was next centrifuged in a Sorvall centrifuge (Model SS-1, Ivan Sorvall, Inc., Norwalk, Conn.) in approximately 40 ml quantities (8 tubes) at low speed for 5 minutes, i.e., Variac (Type 116B, Superior Electric Co., Bristol, Conn.) at 40 volts. The supernatant was discarded. The remaining crude chloroplast was resuspended in buffered sucrose solution using 25 mls per 2 test tubes bringing the total stock to 4 tubes containing 25 mls each. Resuspensions were facilitated by a Vortex mixer (Model M-10715, Thermolyne Corporation, Dubuque, Iowa). These tubes were again centrifuged at 40 volts for 5 minutes, the supernatant discarded and the residue washed and mixed in hypotonic 25 ml glass-distilled water per tube and allowed to stand for 5 minutes. These tubes were centrifuged at high speed (45 volts) for at least 10 minutes and the supernatant discarded leaving a residue that was next extracted with 90 mls of 2/1 (v/v) petroleum ether/methanol solution in the blender at medium speed for one minute. Using two tubes this mixture was centrifuged (Variac at 30 volts) for 10 minutes and the resulting top layer was pipetted off into a dry

round-bottomed flask and evaporated to dryness using a flash-evaporator (Buchler Instruments, Fort Lee, N.J.). This residue was resuspended in 5 mls of 1/1 n-butanol/dodecane and placed in a clean covered storage vial.

Procedure

The bulk BLM bathing medium was 0.1 M acetate titrated with potassium hydroxide to pH 5.1 in laboratory distilled water redistilled in an all-glass still. Preliminary to membrane formation undesirable input currents from the buffer amplifier were offset using the trim adjustment to correct the output signal to zero when the electrodes were shorted. Also, electrode asymmetry potentials typically did not exceed a millivolt. The bimolecular lipid membrane (BLM) was formed by sweeping across the aperture with the tip of a microsyringe after a two microliter extrusion using the repeating dispenser attachment (Tien and Howard, 1972).

Membranes formed in 0.1 M acetate buffer solution thinned to the black condition in approximately ten minutes. This thinning was observed directly using a green filter and dim flash light triggered repeatedly by the timing circuit or more carefully monitored by comparing membrane RC transient times as thinning progressed, as capacitance is inversely related to thickness. Since BLM resistance was measured independently using the voltage divider technique,

$$R_m = R_s \frac{E_m}{E - E_m}$$
, C_m was calculated using R_m and R_s in parallel as the R of RC for the circuit given in Figure 1. The final bilayer lipid

membrane (BLM) exhibited uniform stable resistive and capacitive properties which were measured and recorded since photovoltage features

were determined largely by these characteristic electrical properties. Typical values of R_m and C_m were $10^8 \Omega$ and 5000 pF ($10^6 \Omega\text{-cm}^2$ and $0.5 \mu\text{F/cm}^2$), respectively. Subsequent to membrane stabilization, chemical or pH differences across the chl-BLM were established by the addition of a small volume of concentrated HCl, KOH, FeCl_3 , ascorbate, etc., to the inner chamber with the aid of an Oxford Sampler followed by careful magnetic stirring. A listing of the equipment used follows in Table 1.

TABLE 1
List of Equipment

Item	Model	Manufacturer
Cell assembly Glass cell Teflon cup	Design suggested in Figure 1	Will Scientific Co. Ann Arbor, Mich. 48107
Viewing tube	No. 70266	Edmund Scientific Co. Barrington, N.J. 08007
Microsyringe (100 μ l)	Model PB-600	Hamilton Co., Inc. Whittier, Calif. 90605
Micropipette	Sampler	Oxford Laboratories San Mateo, Calif. 94401
Xenon flashtube assembly	Stroboslave 1539-A	General Radio Co. West Concord, Mass. 01781
Electrodes	Fiber junction calomel, #39270	Beckman Instr., Inc. Fullerton, Calif. 92634
Operational amplifier	Model 1021	Philbrick Nexus Dedham, Mass. 02026
O.A. power supply	MPS-15	Transidyne General Corp. Ann Arbor, Mich. 48103
Dual beam storage oscilloscope	R5031	Tektronix, Inc. Beaverton, Oregon
10^8 to 10^{11} ohm series resistors	Hi-meg resistors	Victoreen Instr. Co. Cleveland, Ohio 44104

CHAPTER IV

RESULTS

Introduction

The microsecond photo-flash illumination of chlorophyll bilayer lipid membranes technique has resolved single-flash voltage responses into clearly defined distinct components representative of kinetically independent membrane photo-processes indistinguishable under continuous illumination circumstances. A variety of combinations of applied voltage, chemical gradients, and pH differences were imposed across the membrane to induce observable effects. Such asymmetries were necessary since, alternatively, excitation would have been randomly partitioned equally to both interfaces, yielding no photoeffect. The voltage transients elicited were in general composed of four processes:

i) a fast, microsecond risetime component induced by electron acceptors such as Fe^{+3} (the Fast Component);

ii) a slower 100 to 300 ms initial phase component in the presence of pH gradient or voltage applied across the membrane (the Slow Component); and two distinct voltage decay kinetics, viz.

iii) a simple 100 to 500 ms RC decay corresponding exactly to the membrane RC transient in the dark; and

iv) a slower decay transient, " λ ", a feature of pH gradient or applied voltage-induced effects only.

These four basic components essentially characterize all the portions of waveforms elicited from chl-BLM (chlorophyll BLM) under

flash excitation regardless of the nature of the trans-bilayer asymmetry. Also, the large difference in component rates has permitted clear delineation of both the fast and slow processes in response to a single flash, facilitating simultaneous evaluation of several components.

The Fast Component

The Fast Component was detected only in response to certain chemical gradients. In the case of FeCl_3 , a maximum photoresponse was elicited at a concentration of 2×10^{-3} M FeCl_3 in the inner ungrounded chamber. The Fe^{+3} chamber potential was driven negative typically 3 to 5 mV upon flash illumination within 10 microseconds, maximum instrumental response rate, and decayed according to the RC exponential transient characteristic of the BLM in the dark (Figure 2). These results were common to all chl-BLM tested. Other electron acceptors, ceric ion and methyl viologen, induced responses of somewhat smaller magnitudes but with similar kinetics; however, since ferric ion was the most effective sensitizer, it was employed in the majority of experiments designed to investigate features of the Fast Component. As previously mentioned, the bathing medium was buffered with 0.1 M acetate and titrated to pH 5.1.

The Fast Component and accompanying RC decay appeared alone only in the total absence of applied voltage or pH gradient; otherwise the Slow Component appeared to some extent. This presented moderate experimental difficulties, viz. FeCl_3 in aqueous solution is an electron pair acceptor and hence a Lewis acid. Although the inner chamber was buffered with 0.1 M acetate, FeCl_3 decreased the inner


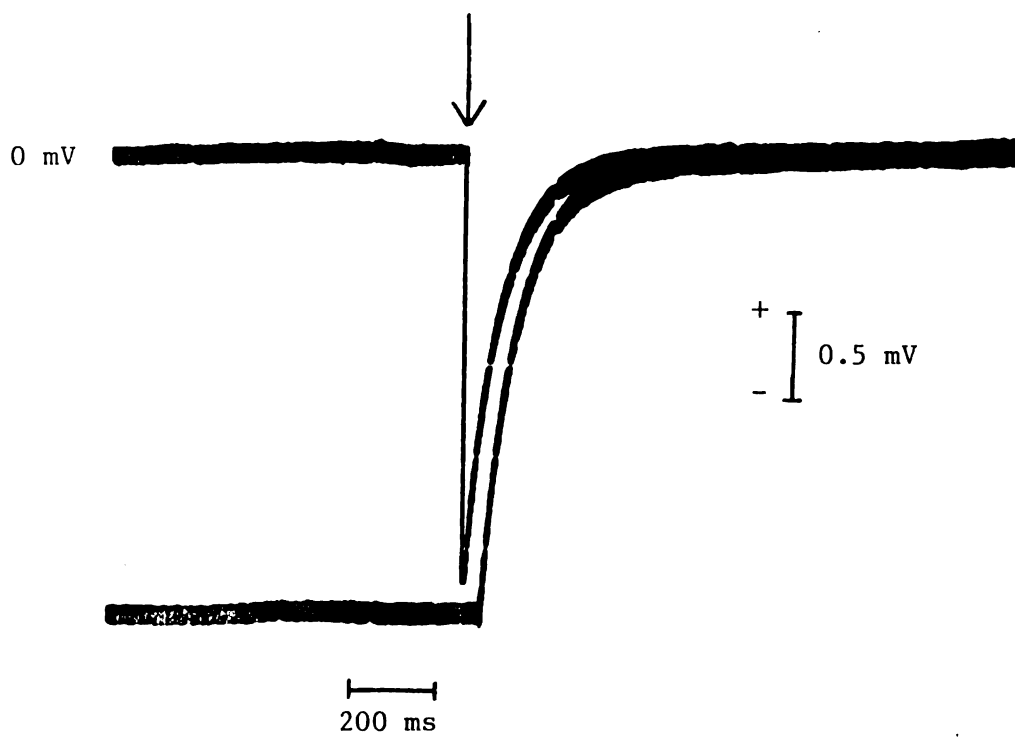


Figure 2. Flash response in the presence of 10^{-2} M FeCl_3 in the inner chamber compared to the dark chl-BLM RC transient. Arrow denotes flash.



chamber pH typically 0.2 units, imposing a small pH gradient across the chl-BLM and inducing therefore slight Slow Component character in the response waveform. The Slow Component contribution, usually essentially insignificant, could be additionally minimized in most cases via the external application of a slight reverse biasing potential.

A distinctive feature of the Fast Component was the fact that maximum possible applied voltages of ± 70 mV, corresponding to $\pm 70,000$ Volts/cm field strength within the chl-BLM did not alter the polarity of the fast response; it continued to exhibit a polarity indicative of negative charge flow to the ferric/chl-BLM interface. The magnitude of the response was altered $\pm 15\%$ under application of these intense fields, augmented when the field was of a polarity to assist negative charge flow to the ferric/chl-BLM interface and diminished when the field was oriented to retard current flow to this interface.

The Slow Component

Upon flash excitation the Slow Component appeared in the presence of applied voltages or transmembrane pH differences. Its risetime was on the order of 0.5 seconds and its polarity in the case of applied voltage was such that the absolute magnitude of potential across the BLM in the dark prior to flash was reduced. Also, the flash response amplitude was directly proportional to the potential applied. An example of the addition of a positive Slow Component to a negative iron-induced Fast Component when a negative potential is applied is given in Figure 3.

The magnitude of the Slow Component light response was increased by the addition of bromide or iron in equal concentrations to both sides of the membrane. This concentration symmetry minimized fast effect contributions to the photoresponse, facilitating study of the Slow Component alone. It was found that FeCl_3 , in addition to inducing the large fast photoresponse described earlier also enhanced the kinetically independent slow response approximately twentyfold at 10^{-4} M concentrations. Bromide also enhanced the Slow Component photovoltage magnitude somewhat (Figure 4). The pH gradient-induced photoresponse exhibited kinetics similar to those of the applied voltage response but its polarity was always negative with respect to the high pH side of the membrane.

Lambda Decay

Whereas the Fast Component was discharged at a rate given by the chl-BLM RC time, the Slow Component invariably returned to the dark voltage at a much slower rate. Figure 5 compares an RC transient with a voltage gradient-induced rapid repeated flash photoeffect decay process for the same membrane. This multi-flash technique yielded a better-resolved decay process than attainable using single flash excitation. Clearly, the rates are not the same. The rate constant for this decay, λ , was typically 2 sec^{-1} while the RC rate constant was 5 sec^{-1} . (This corresponds to a 200 ms "RC time".) Though λ varied from one chl-BLM to another within values of 0.5 to 2.5 sec^{-1} , for any single membrane λ remained constant and was not a function of time, applied voltage, total membrane illumination time or membrane resistance values.


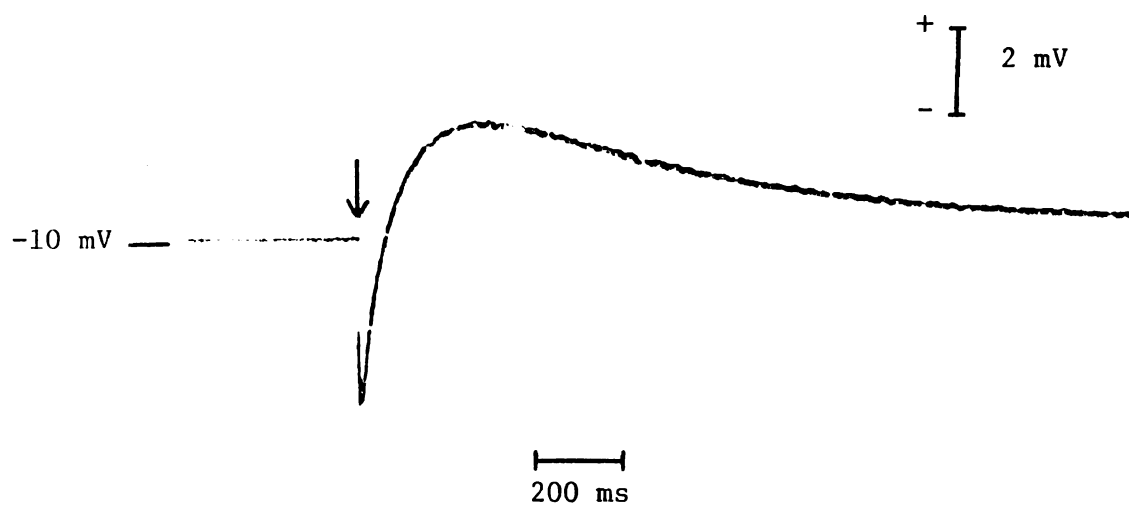


Figure 3. Biphasic response in the presence of FeCl_3 and negative applied voltage.




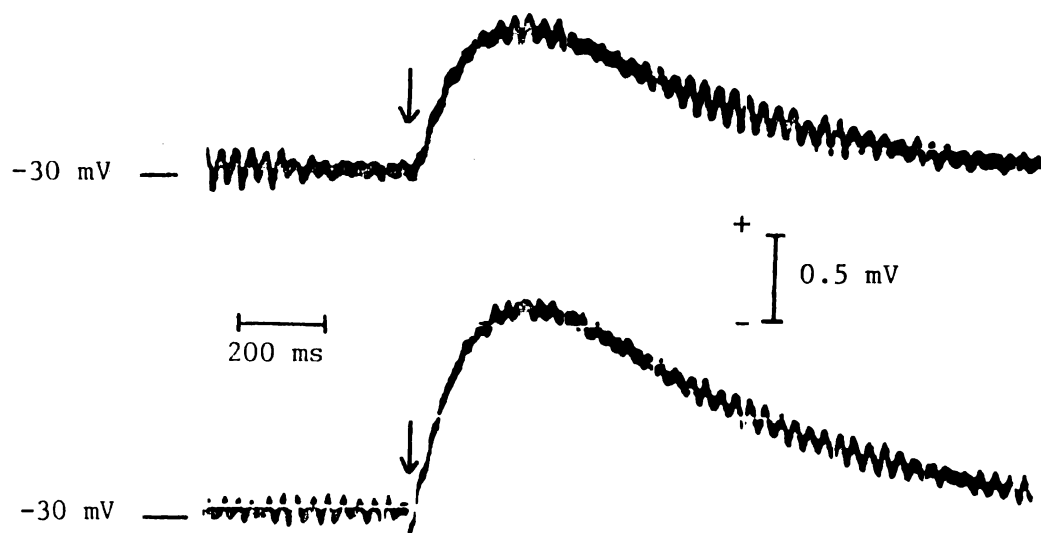


Figure 4. Top trace: Slow Component in the presence of applied voltage only.

Bottom trace: enhanced photovoltage transient subsequent to the addition of 0.023 M NaBr.




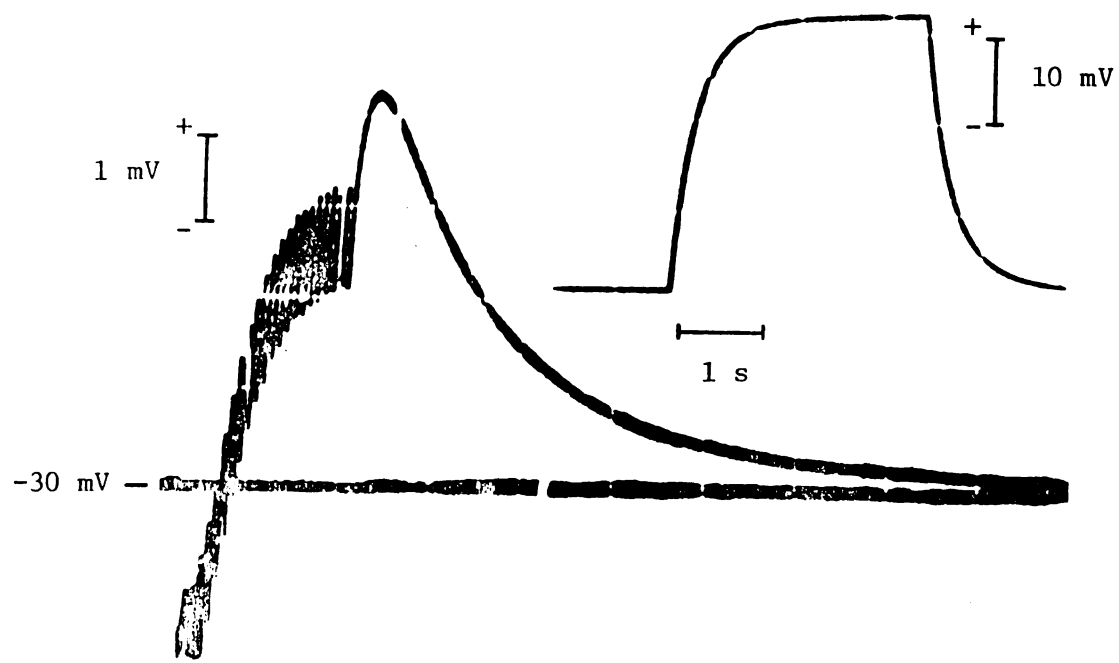


Figure 5. Chl-BLM Slow Component decay kinetic (left) compared to membrane RC transient (right).



The Quenching Phenomenon

Certain compounds were found to eliminate completely or "quench" the pH or voltage-induced slow response without modifying the Fast Component. In order of quenching effectiveness, these include: ascorbic acid, tannic acid (dicatechin), p-benzoquinone, and sodium azide. The quenchers exhibited identical quenching properties in either single chamber or both chambers. Ascorbate at 10^{-3} M eliminated the Slow Component immediately upon addition prior to stirring, as seen in Figure 6, while at 10^{-4} M 20 seconds of stirring was necessary in order for a similar degree of quenching to be observed. Figure 7 compares the relative quenching efficiencies of ascorbic acid and sodium azide. The quenching phenomenon was essentially irreversible for any single BLM; i.e., once quenched the Slow Component did not reappear.

Figure 8 demonstrates quencher elimination of a bromide-enhanced slow response while Figures 9 and 10 illustrate the ability of tannic acid and ascorbate, respectively, to quench slow responses of both polarities. These results were independent of which chamber contained the quenching agent.

Further, the light and dark current-voltage characteristics of chl-BLM in the presence and absence of Slow Component quencher were measured and are shown in Figure 11. As indicated, after the addition of quencher, the I-V characteristics of the membrane were identical in both the dark and upon illumination.

Figure 6. Top trace: immediate elimination of the Slow Component upon addition of 10^{-3} M ascorbate (indicated by noise);

Bottom trace: gradual disappearance of the slow transient in the presence of 10^{-4} M ascorbate.

11

Figure 7. Top traces 1 and 3: biphasic responses in the absence of quencher;

Bottom traces 2 and 4: reduced Slow Component in the presence of 2×10^{-3} M NaN_3 (trace 2) and 2×10^{-3} M ascorbate (trace 4).




Figure 8. Quencher elimination of a bromide-enhanced slow response.

Trace 1: applied voltage only.

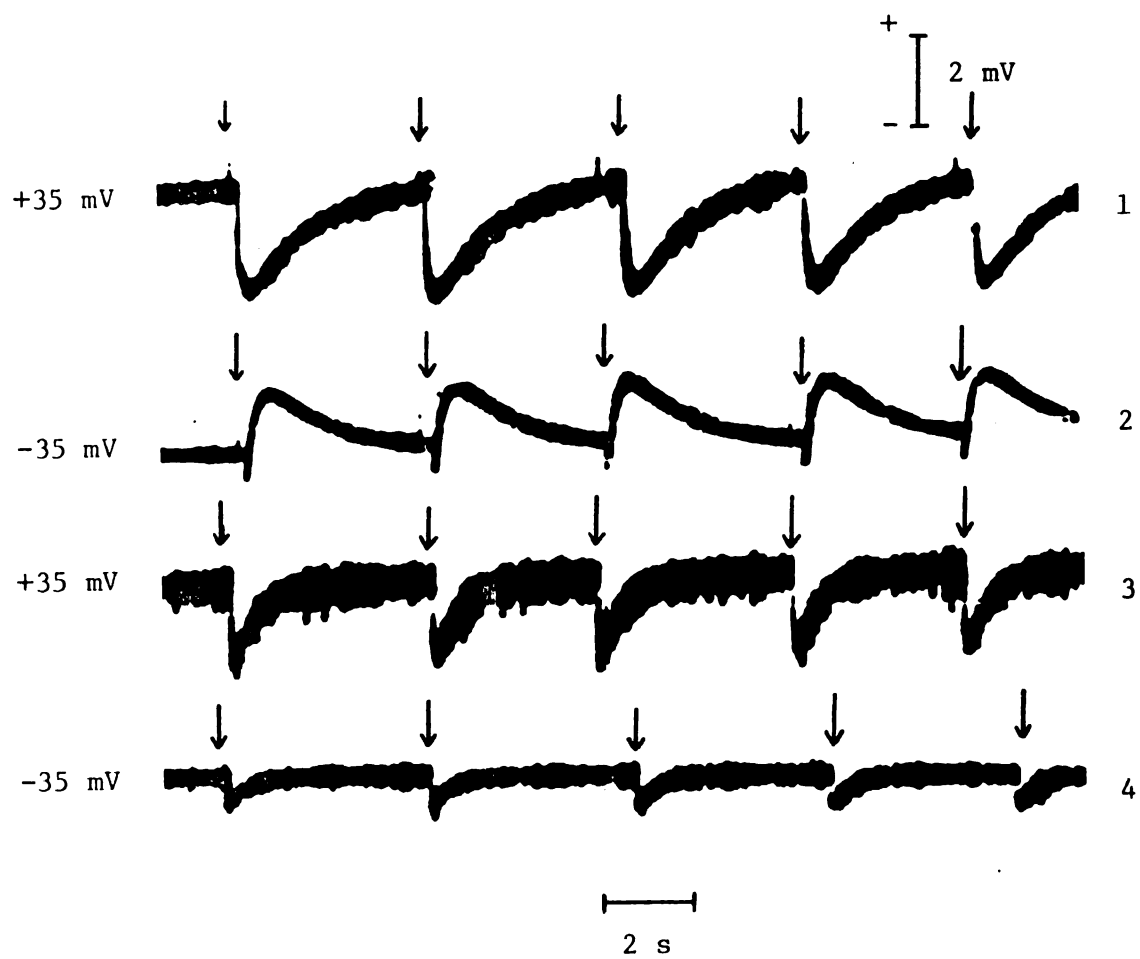
Trace 2: enhancement in the presence of bromide.

Trace 3: no response after 10^{-3} M ascorbate addition.

Figure 9. Slow transient quenching by 10^{-3} M tannic acid while 10^{-3} M FeCl_3 -induced Fast Component remains unmodified.

Traces 1 and 2: prior to tannic acid addition.

Traces 3 and 4: subsequent to tannic acid addition.






Figure 10. Quenching by 10^{-3} M ascorbate in the presence of repeated flash illumination (~ 50 Hz). Equal applied voltages of opposite polarity provide the only asymmetry across the membrane. The noise spike indicates addition of quencher; subsequently the chl-BLM is rendered relatively light-insensitive.


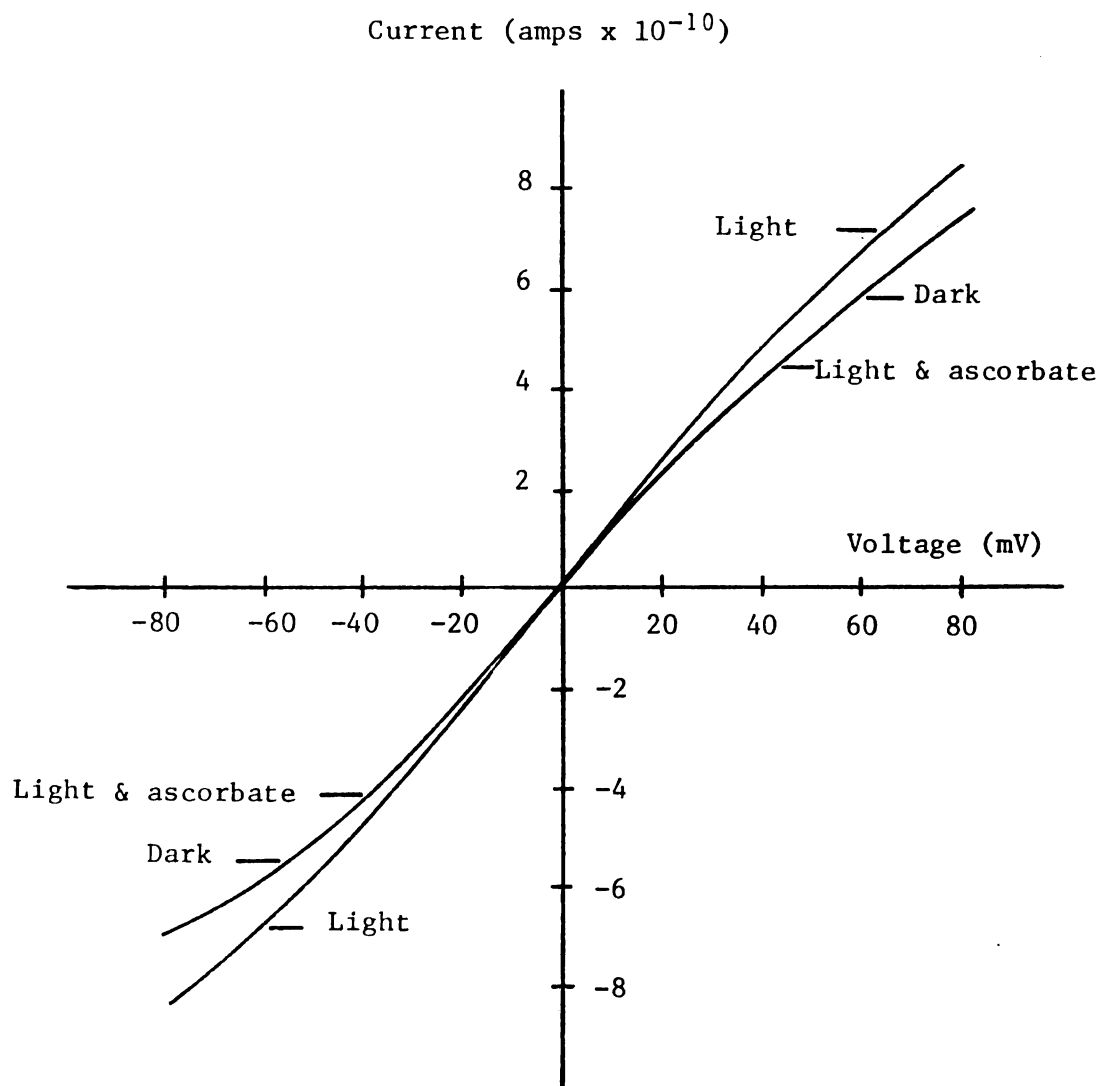


Figure 11. Light and dark current-voltage relationship of chl-BLM prior and subsequent to the addition of 10^{-3} M ascorbate.



CHAPTER V

DISCUSSION

As an ultrathin ($\sim 10^{-6}$ cm), relatively large surface area, low dielectric-constant partition between highly conducting aqueous phases, the chl-BLM possesses an appreciable electrical capacitance, usually $\sim 5 \times 10^{-9}$ F or 5000 pF (C_m). Additionally, the 1 mm^2 membranes employed in these investigations exhibited electrical resistances of $1 \times 10^7 \Omega$ to $5 \times 10^8 \Omega$ (R_m). The BLM, then, is electronically equivalent to a capacitor shunted with a resistor; it is, in effect, a "leaky" capacitor. As any voltage is applied to this system, either through an external voltage source or via the action of light, the voltage transients appearing across the effective membrane R_m , C_m combination obey the following relationship: as the membrane capacitance C_m charges and discharges, the BLM exhibits voltage transients given by $V(t) = V_o(1 - e^{-t/RC_m})$ and $V(t) = V_o(e^{-t/RC_m})$, respectively, where V_o is the maximum voltage appearing across the BLM in either case, $V = Q/C_m$, and most importantly, R is the Thevenin equivalent resistance with respect to C_m (Korneff, 1968). For the chl-BLM this value is given by R_m in parallel with the internal or series resistance of the EMF shunted across the membrane; i.e., $R = R_s R_m / (R_s + R_m)$. In the simple case of a voltage discharge when the charging element has been removed, R_s is nearly infinite and thus $R = R_m$ and the discharge rate constant is simply $1/R_m C_m$, typically 5 sec^{-1} . For a

potential applied through a resistance R_s of $10^8 \Omega$, R becomes $5 \times 10^7 \Omega$ ($R_m = 10^8 \Omega$) and the charging rate constant is equal to 10 sec^{-1} .

The chl-BLM flash-elicited voltage waveform in the instance of an imposed transmembrane chemical gradient of FeCl_3 indicates rapid negative charge flow to the chl-BLM/ FeCl_3 interface that rapidly ($<1 \text{ ms}$) charges the BLM capacitance followed by the total disappearance of charging current flow resulting in discharge of the membrane capacitance in precisely the same kinetic manner as C_m is discharged in the dark according to membrane $R_m C_m$ characteristics. The rapid initial phase voltage transient represents charge separation across the membrane by a current-delivering element not hindered by high internal resistance. The condition in which charge separation can be established across the chl-BLM capacitive element within only 1 ms is that the input Thevenin equivalent resistance be reduced to less than $10^5 \Omega$, yielding an RC charging time of less than 0.5 ms . The experimental decay of the Fast Component is seen to be kinetically equivalent to the $R_m C_m$ transient exhibited by the chl-BLM in the dark when the charging element is suddenly removed (cf. Figure 2); i.e., the Thevenin equivalent resistance is again simply R_m . Figure 12 illustrates an electronic circuit voltage waveform response to a brief introduction of a current-generating element.

This analysis, then, indicates that a transmembrane current of typically $\sim 10^{-8}$ amps flows to the membrane capacitance upon flash excitation in the case of FeCl_3 -induced fast responses. This value is corroborated by actual short circuit current measurements (cf. p. 83). These data support the view of Tien and Huebner (Tien and Huebner, 1973)


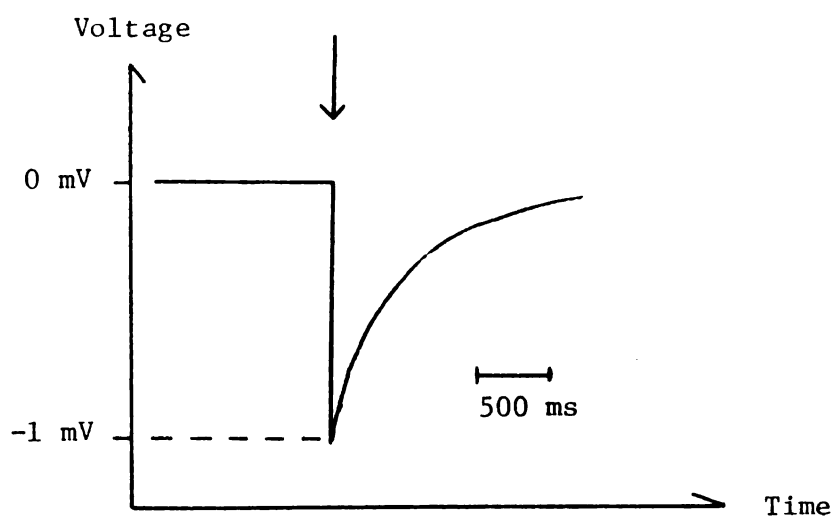
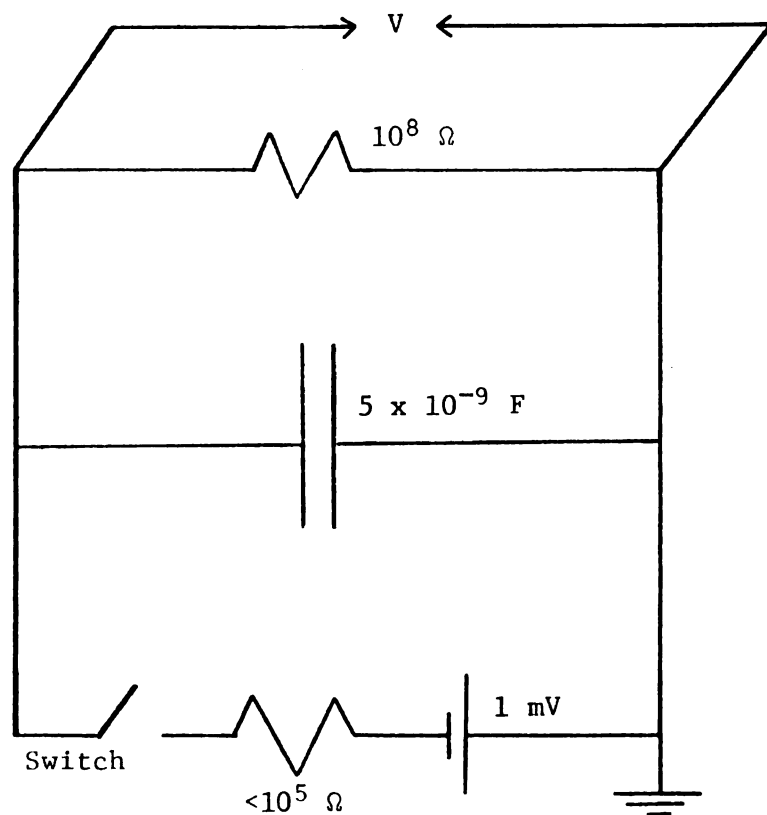


Figure 12. RC system analogous to chl-BLM and voltage waveform for switch closed 1 ms (denoted by arrow). The charging rate constant is greater than 2000 sec^{-1} , corresponding to an RC time of less than 0.5 ms; and the discharge rate constant is 2 sec^{-1} , corresponding to an RC time of 500 ms (cf. Figure 2).



that the chlorophyll molecule excited by light to a reduction potential more negative than that of the $\text{Fe}^{+3}/\text{Fe}^{+2}$ reduction-oxidation couple may donate an electron to the ferric (Fe^{+3}) ion, the oxidized chlorophyll subsequently oxidizing and being reduced by substrate, most likely H_2O , at the opposing interface. These coupled oxidation-reduction reactions driven by the photoenergy harvested by the chl-BLM imply a net electron flow to the $\text{FeCl}_3/\text{chl-BLM}$ interface. After illumination and the charging of C_m due to this current flow, the decay process follows $R_m C_m$ exponential decay kinetics, indicating that light-stimulated redox processes have ceased; indeed, the capacitance dissipates this accumulated charge precisely as it does any charge added to it in the dark.

In addition, these decay kinetics illustrate that the membrane capacitance becomes charged and thus the initial photo-stimulated charge flow must be a transmembrane one, not merely an electrical double-layer charging current localized at a single interface.

As demonstrated above, the shape of the voltage transient responding to flash excitation in the case of FeCl_3 -induced effects provides specific information concerning the current-generating nature of the fast photoresponse. Consequently a study of features of the Slow Component response elicited in the presence of voltage gradients follows. Transient responses in the case of pH gradients displayed waveforms kinetically identical to applied voltage responses; therefore applied voltages were employed in the majority of experiments investigating the slow response, eliminating several limitations and precautions necessary in the pH gradient instances, viz.: applied voltages were easily varied or removed and reapplied during experiments

while pH gradients could not so easily be varied or eliminated; chl-BLM functions as a hydrogen electrode, exhibiting the hydrogen ion Nernst potential in the dark and this "dark potential" invariably introduced a voltage bias requiring difficult normalization of data; and also pH differentials were likely to result in membrane surface asymmetries.

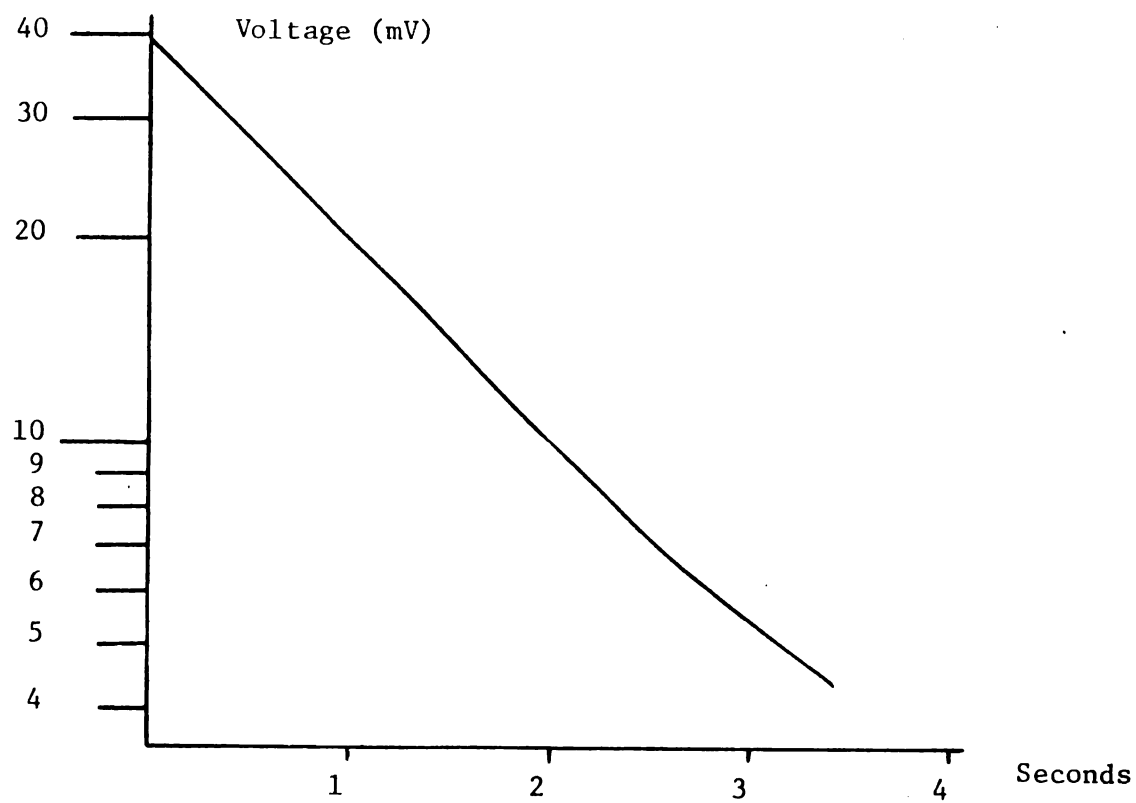
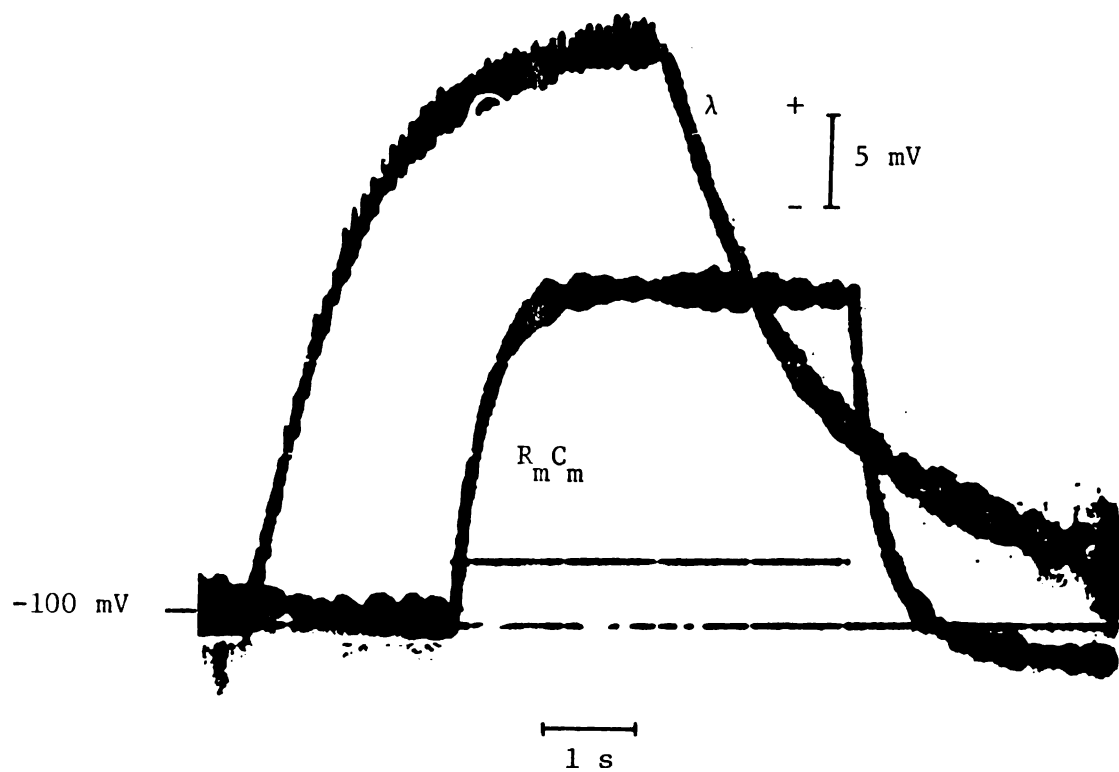
Initially the slow response decay process was examined. As pointed out earlier, the rapidly repeating flash illumination approach was optimal for this investigation as it provided a large amplitude photoresponse concomitant with long-lived easily-resolved decay. It will be shown later that the decay waveform is not altered by the number of flashes incident upon the membrane prior to decay. The results are indicated in Figure 13. Significantly, the decay process was found to be a simple first order exponential one. That is, for the beginning of decay at $t = 0$,

$$V(t) = V(0)e^{-\lambda t}$$

where λ (lambda) is the rate constant. Although for different chl-BLM λ varies from 0.5 sec^{-1} to 2.5 sec^{-1} , corresponding to $1/e$ times (duration of time in which V falls to V/e or $0.368 V$) of 2000 ms and 400 ms, respectively, λ remains essentially constant for any single BLM.

A major point is that λ is not equal to or a function of $R_m C_m$; λ is always greater than $(R_m C_m)^{-1}$. In other words, λ decay is always slower than $R_m C_m$ decay, as exemplified in Figures 5, 13, 15, and 16. An earlier model for this Slow Component assumed $R_m C_m$ decay resulting in the problem that "the theoretical voltage. . . falls too rapidly after the peak value" (p. 71, Tien and Huebner, 1973).

Figure 13. Experimental Slow Component decay (λ) and plot of $\log V$ values versus time. The linearity of this plot demonstrates the first order exponential character of the decay. ($R_{m m} C_m$ decay is again included for purposes of comparison.)



The next step in the effort to describe mathematically the entire experimental waveform was to assume the most likely, simplest case for the initial phase of the response: that it is also a first order exponential process. In the idealized absence of decay and for strobe flash at $t = 0$,

$$V(t) = V_o (1 - e^{-Kt})$$

where V_o is the voltage value at $t = \infty$.

Whether this assumption holds for experimental waveforms was determined in the following manner: if the initial phase is first order exponential,

$$V(t) = V_o (1 - e^{-Kt})e^{-\lambda t}$$

will accurately describe the entire waveform. The constant λ was measured experimentally and K was determined numerically for experimental waveform sets of values of V and t . This computation was facilitated by taking the first derivative of $V(t)$ with respect to time and measuring the experimental time interval from $t = 0$ to the moment of peak voltage, t_{Max} . Thus

$$K = \lambda (e^{Kt_{\text{Max}}} - 1).$$

Now for any t ,

$$V(t) = V_o (1 - e^{-Kt})e^{-\lambda t}$$

yields a voltage value that may be compared with the experimental voltage at that instant. The fit achieved is quite good, as shown in Figure 14. The fact that λ values derived from rapid repeating flash illumination provide accurate fits to single flash waveforms is clear indication that the decay form is not altered by the number of flashes incident upon the membrane prior to decay.

Figure 14. Experimental chl-BLM slow response waveform

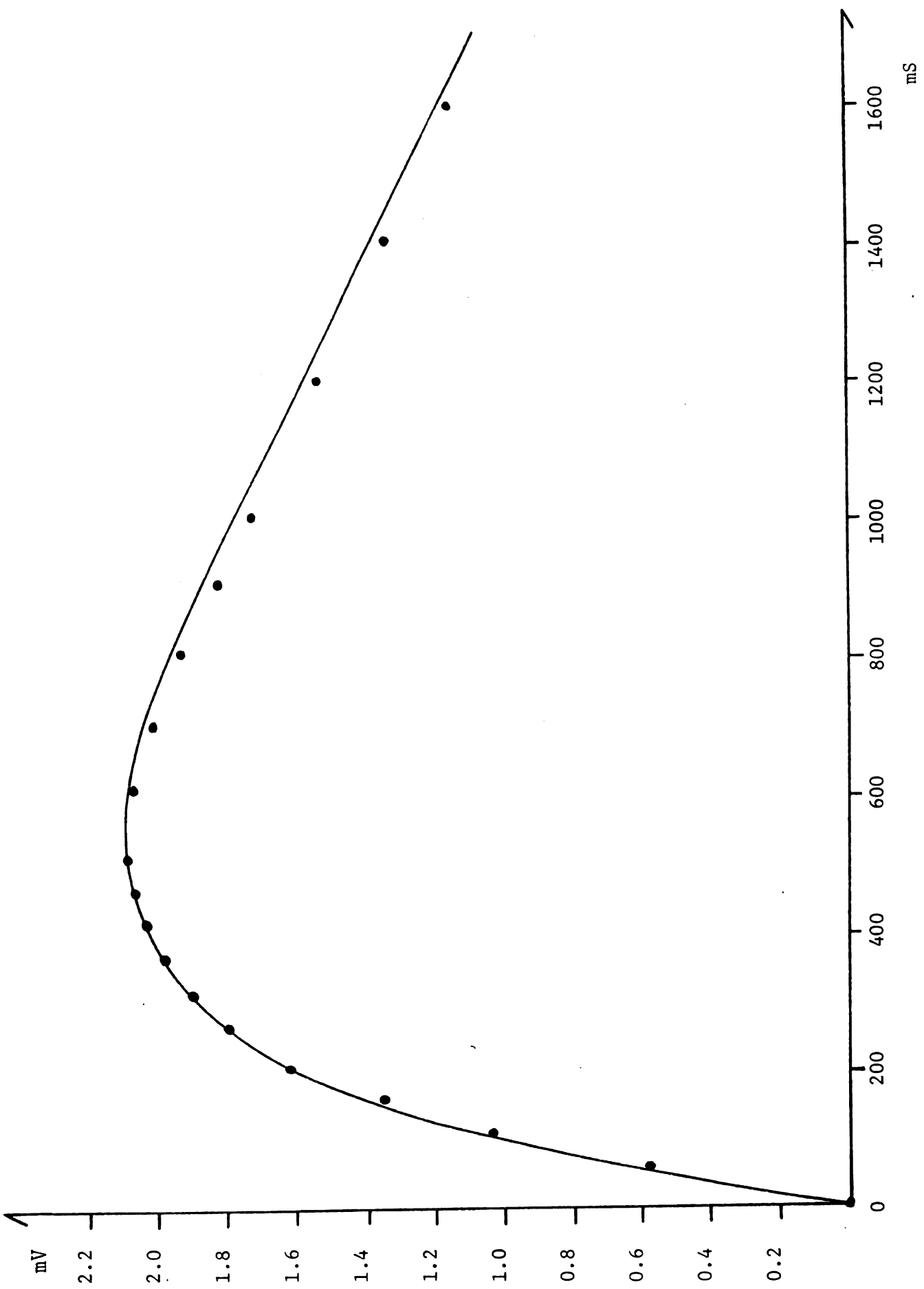
and points predicted from $V(t) = V_o(1 - e^{-Kt})e^{-\lambda t}$
approximation.

For this membrane:

$$K = 3.68 \text{ sec}^{-1}$$

$$\lambda = 0.69 \text{ sec}^{-1}$$

$$V_o = 3.53 \text{ mV.}$$



In the course of verifying this Slow Component fit for several chl-BLM, it was noticed that the constant K for a particular membrane was invariably equal to $(R_m C_m)^{-1}$ for that BLM. This observation introduced distinct advantages: the numerical method for solving for the value of K could be abandoned and chl-BLM Slow Component waveform shapes could be predicted exactly, prior to any flash illumination with λ having been measured from continuous illumination response decay and $K = (R_m C_m)^{-1}$ having been determined in the dark, as shown in Figures 15 and 16.

Further, from

$$V(t) = V_o (1 - e^{-Kt}) e^{-\lambda t}$$

setting $\frac{dV(t)}{dt} = 0$ when $t = t_{\text{Max}}$, yields

$$t_{\text{Max}} = \frac{\ln\left(\frac{K + \lambda}{\lambda}\right)}{K} \text{ sec.}$$

This expresses the voltage waveform peak time in terms of λ and $(R_m C_m)^{-1}$. As a test of this prediction, external resistances were shunted across the chl-BLM, effectively changing R_m and consequently also t_{Max} . Figure 17 indicates experimental peak times altered precisely as expected. The successful prediction of experimental waveform shapes justifies the original assumptions and provides a basis for identification of the photo-stimulated membrane events responsible for the chl-BLM Slow Component response to flash illumination. The current-voltage relationships of the membrane in the dark and upon illumination (Figure 11) together with the fact that the initial growth phase of the Slow Component exhibits a $(R_m C_m)^{-1}$ rate constant constitute compelling evidence that the Slow Component is a

Figure 15. Slow Component waveforms and points calculated using $R_{m m} C_m$ and λ data included in photographs.

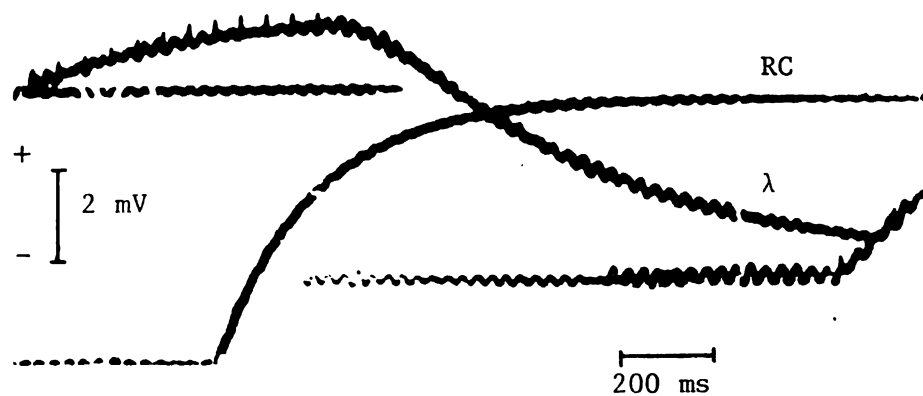
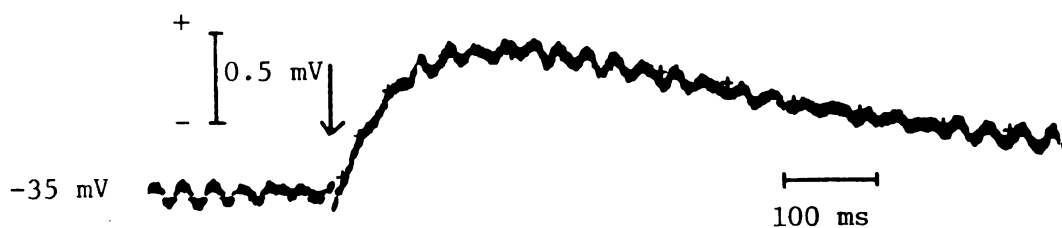
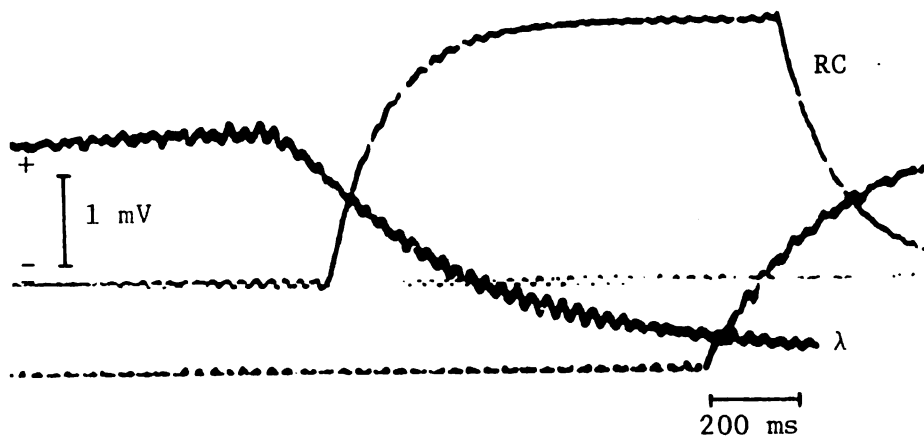


Figure 16. Additional Slow Component waveforms and points
calculated from $R_{m m} C_m$ and λ data included in
photographs.

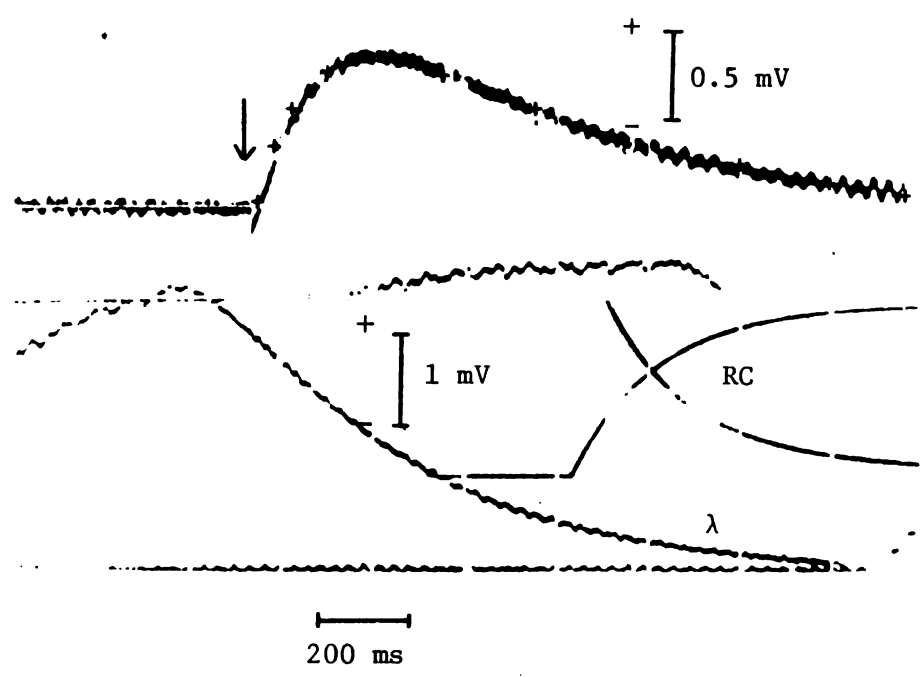
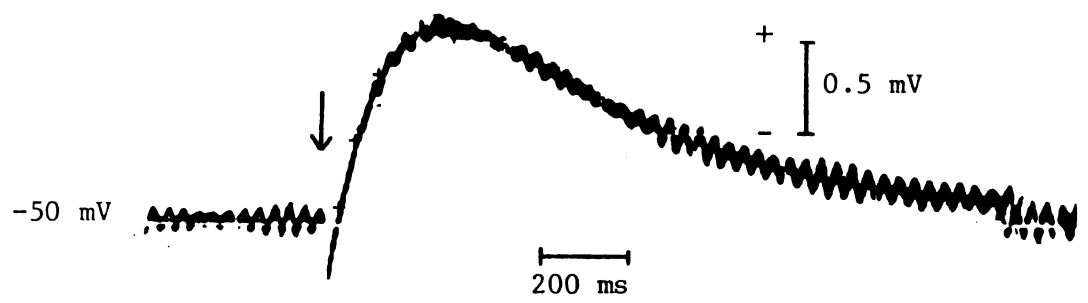
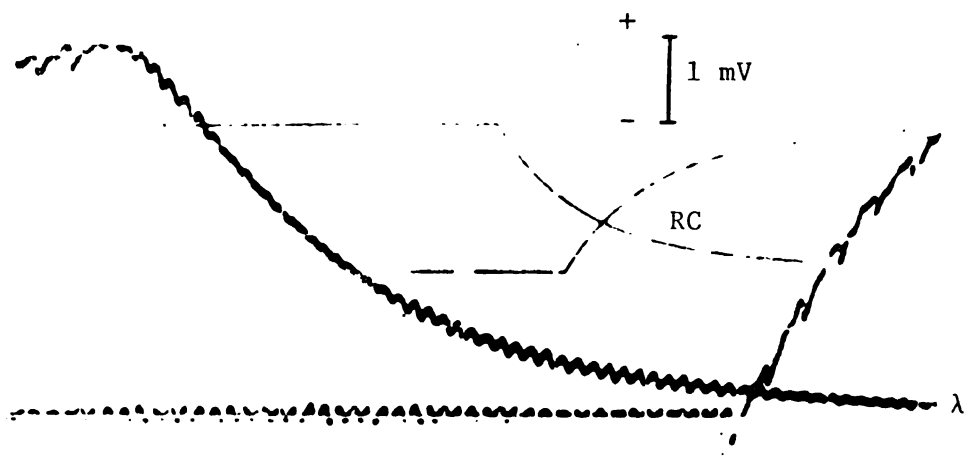


Figure 17. Slow Component peak time, t_{Max} , dependence upon effective R_m . In both cases

$$t_{\text{Max}} = \frac{\ln\left(\frac{K + \lambda}{\lambda}\right)}{K} \text{ sec},$$

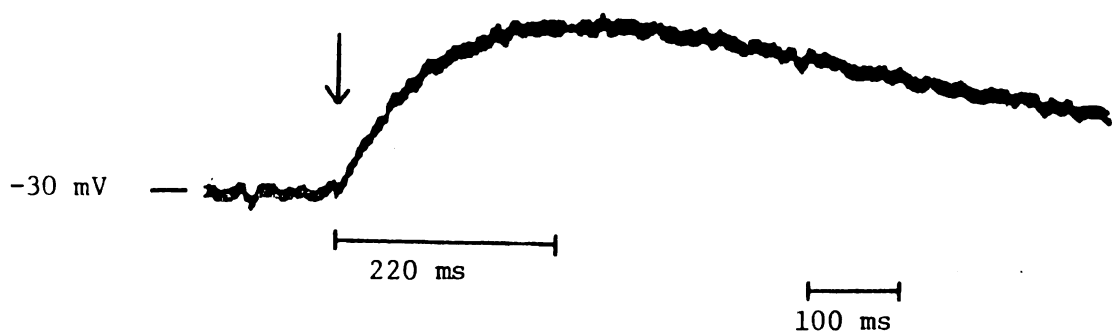
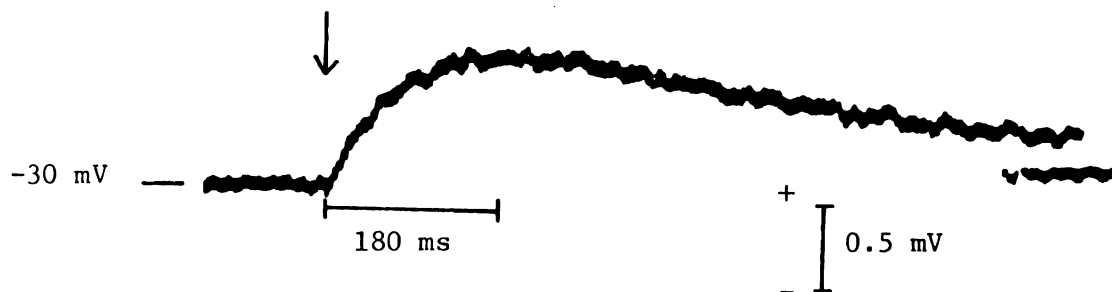
$$C_m = 3 \times 10^{-9} \text{ F and } \lambda = 1.9 \text{ sec}^{-1}.$$

$$\text{Upper trace: } R_m = 3.21 \times 10^7 \Omega \text{ (} R_s = 9 \times 10^7 \Omega \text{);}$$

$$\text{calculated } t_{\text{Max}} = 180 \text{ ms.}$$

$$\text{Lower trace: } R_m = 4.76 \times 10^7 \Omega \text{ (} R_s = 1 \times 10^9 \Omega \text{);}$$

$$\text{calculated } t_{\text{Max}} = 221 \text{ ms.}$$

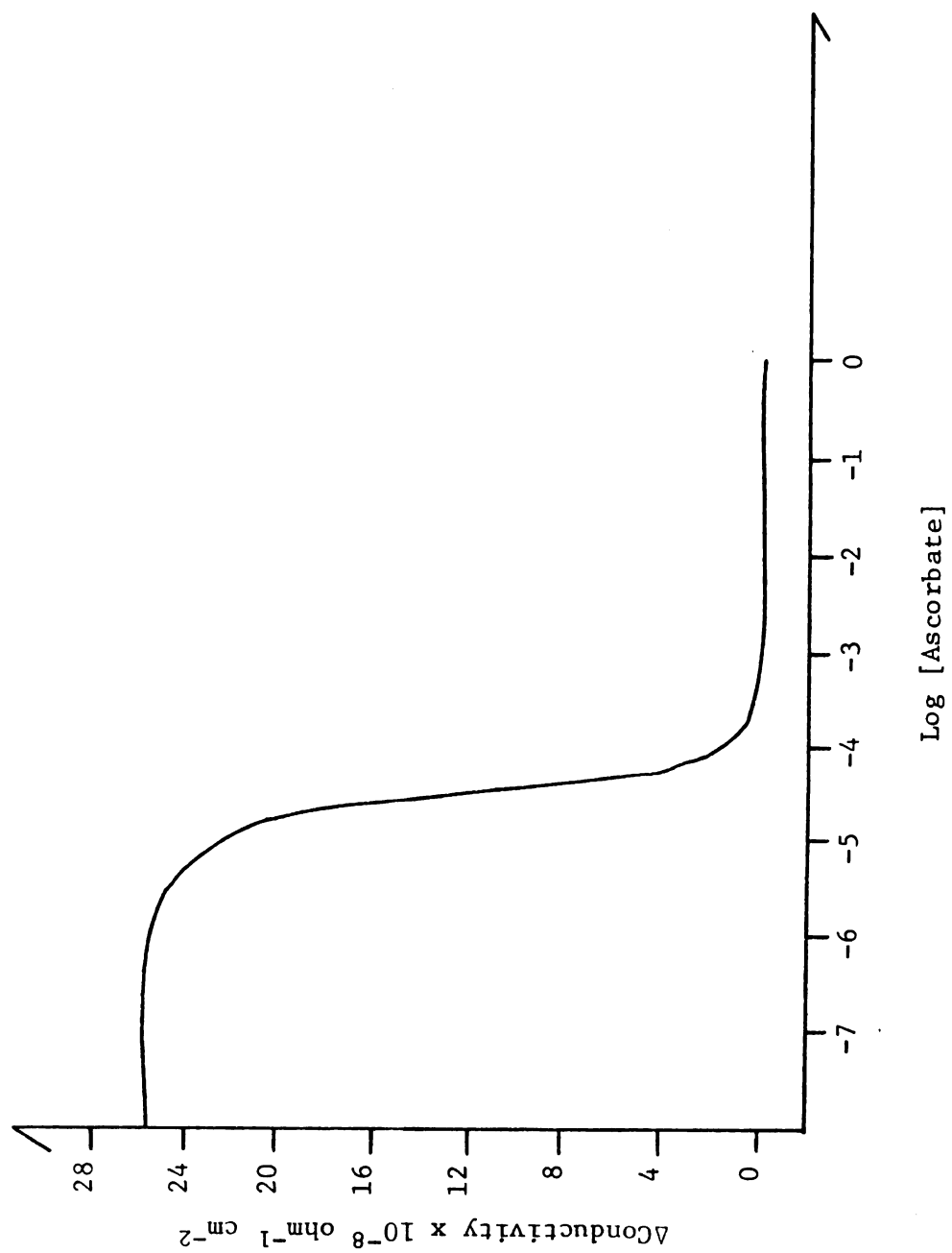


result of chl-BLM conductivity enhancement upon illumination. All of the results are in accord with this interpretation.

That this conductivity enhancement or resistance decrease is 3% at most accounts for the fact that $R_m C_m$ values measured in the dark were sufficiently close to the slightly (<3%) smaller $R_m C_m$ values actually characteristic of the membrane upon illumination that excellent fits were obtained regardless. Note in Figure 14 that the experimental voltage increase is very slightly more rapid than the rise predicted according to the dark $R_m C_m$ values. The sudden introduction of slight additional conductivity across the membrane simply decreases the voltage dropped across the BLM, whose resistance in relation to the fixed shunt resistance determines the amount of transmembrane potential. This transmembrane potential decrease would be expected to display $R_m C_m$ kinetics. The λ decay of the Slow Component, the first order exponential return to the dark resistance value, is slower than the $R_m C_m$ transient and hence is not at all modified by the membrane $R_m C_m$ components.

The quenching phenomenon, then, represents an elimination of light-induced conductivity enhancement. An ascorbate concentration versus photoconductivity quenching ability profile is given in Figure 18. Since prior to quencher addition the enhanced conductivity decays with rate constant λ of $\sim 2 \text{ sec}^{-1}$, a metastable state of lifetime $\sim 500 \text{ ms}$ is responsible. Recognizing that the conductivity enhancement action spectrum correlates with the chlorophyll absorption spectrum, that the chlorophyll triplet excited state may possess lifetimes of this duration (Vernon and Seely, 1966), that Slow Component enhancers iron and bromide enhance also excited singlet to triplet intersystem crossing

Figure 18. Transient BLM photoconductivity dependence upon quencher concentration. Dark conductivity = $\sim 1.5 \times 10^{-6} \text{ ohm}^{-1} \text{ cm}^{-1}$.



(McGlynn, 1969), that the slow transient quenchers ascorbate and p-benzoquinone are reported to be excellent in vitro chlorophyll triplet quenchers (Livingston, 1960; Fujimori, 1957; Livingston, 1963), and that at concentrations of chlorophyll likely in the chl-BLM (Alamuti and Luger, 1970) chlorophyll triplet states would be expected to decay in a first order exponential manner (Vernon and Seely, 1966), it is reasonable to suppose that photo-populated chlorophyll triplet states are responsible for the conductivity enhancement in chl-BLM manifested as the Slow Component. In addition, the fact that there exists a pH gradient-induced Slow Component suggests that the chlorophyll triplet conductivity channels are relatively specific for protons.

The Fast Component represents a current delivering process at a polarity fixed only by the arrangement of redox agents; the Slow Component represents a conductivity increase with kinetic features containing information concerning chlorophyll metastable states in chl-BLM.

CHAPTER VI

ADDITIONAL RESULTS

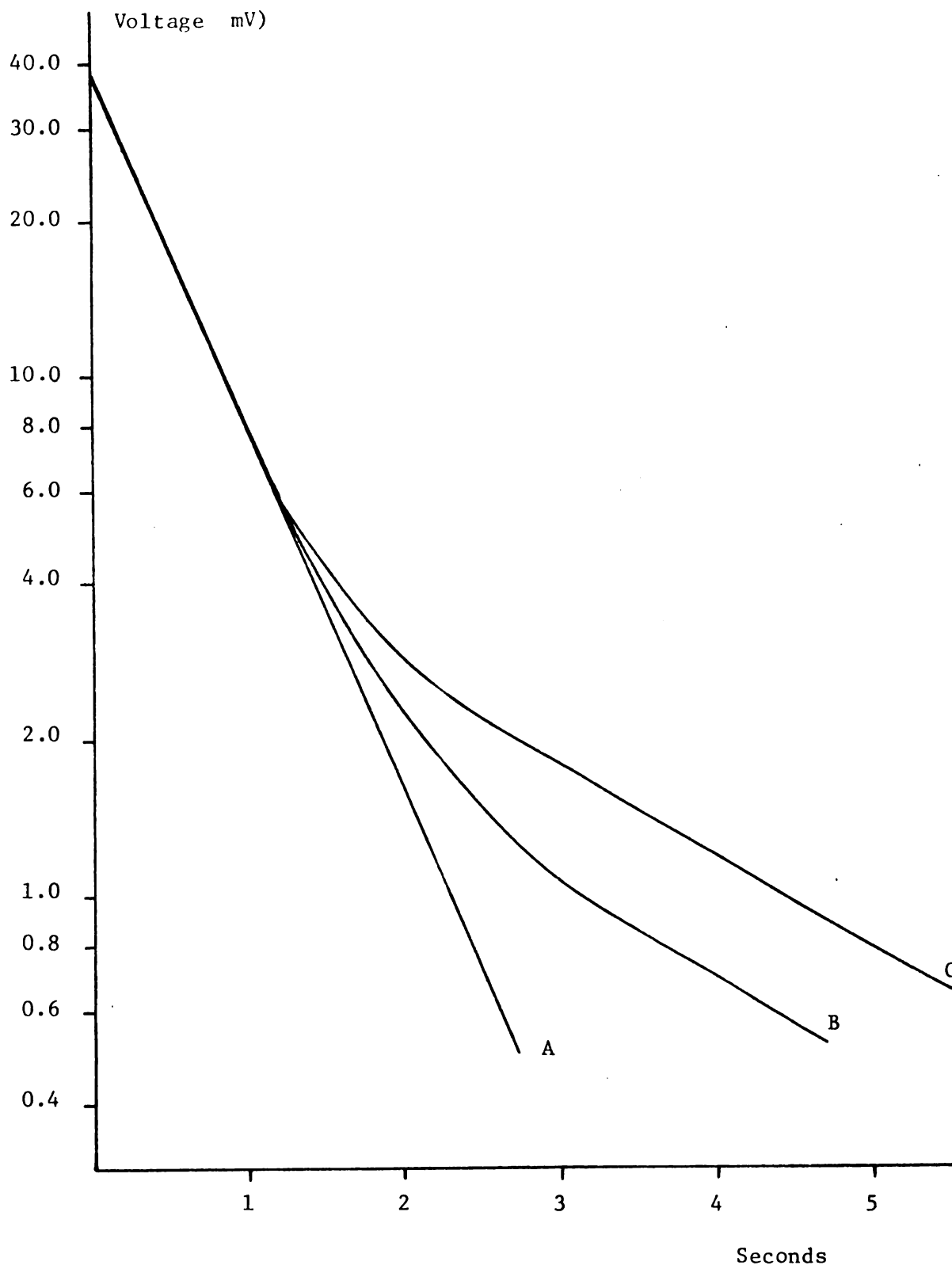
Dual Component Voltage Decay

In the course of the measurement of dark $R_m C_m$ values for chl-BLM it was observed that the $R_m C_m$ transients in most cases followed exactly the logarithmic decay pattern expected from the membrane as detailed on page 47 of this thesis. However, decay transients from potentials applied longer than 5 seconds exhibited a slower decay contribution whose magnitude was directly dependent upon the duration of voltage application. Figure 19 illustrates the appearance of this secondary decay. The linearity of the secondary portion indicates the exponential character of this transient. Also, voltages applied for periods longer than ~ 20 seconds induced secondary contributions no greater than that characteristic of the 20 second applied potential case and as indicated this maximum secondary decay does not appear until V has fallen to $\sim V_o/10$, accounting for the accuracy of the $R_m C_m$ approximation of this decay waveform.

When an impressed potential induces charge flow across the membrane, the most permeable charge carriers may accumulate in the region of the interface to which they are driven. If so, upon removal of the applied field these permeable charges may simply diffuse across the chl-BLM according to their concentration gradient, resulting in an exponentially decaying voltage of a polarity tending to sustain the

Figure 19. Logarithmic plots of chl-BLM voltage decays for potentials applied.

- A. 0 seconds (pulse). Simple $R_m C_m$ exponential as expected.
- B. 6 seconds. Another slower first order decay becomes apparent.
- C. 20 seconds. Maximum secondary decay contribution.



transmembrane potential drop that existed during external voltage application.

Chl-BLM Mechano-Electric Oscillations

When the chl-BLM support cell was vibrated at uniform frequencies, the membrane responded with mechanical oscillations, from the planar to alternately nearly hemispherical configurations in each chamber, at a frequency identical with the driving vibration. Interestingly, this mechanical oscillation was accompanied by a membrane ± 1 mV electrical oscillation of the same period.

The stroboscope trigger rapid repeated dim flash mode was employed to determine membrane mechano-electric oscillation frequencies and, further, to establish the correlation between polarity of voltage and direction of membrane distortion with respect to the electrically grounded chamber; only when the flash frequency was tuned to equal the chl-BLM vibrational frequency, flash-denoting spikes were distributed on the BLM voltage output display at one spike per electrical oscillation, and the membrane mechanical vibration was visually totally arrested. Simply, the chl-BLM was being illuminated at only one particular moment in each of its vibrational cycles, giving the visual appearance of no movement. The synchronous strobe flash frequency, typically ~ 30 Hz, was then altered slightly, introducing a phase difference resulting in very slow apparent membrane vibration. A mark was easily made at the moment the chl-BLM appeared maximally distended into the ungrounded electrode chamber (Figure 20), and the strobe spike, then, indicated the polarity of membrane potential at this configuration by its position on the voltage waveform.

The chl-BLM potential was established in this manner to be negative when the membrane is distorted toward the ungrounded electrode compartment.

As a possible explanation: for the hemispherical configuration of a 100 \AA (10^{-6} cm) thick bilayer of planar diameter 1 mm (0.1 cm), the inner radius, R_i , is 0.05 cm or $5 \times 10^6 \text{ \AA}$ while the outer radius, R_o , is 0.050001 cm or $5.0001 \times 10^6 \text{ \AA}$. So the area difference is given by

$$\Delta A = 2\pi(R_o^2 - R_i^2) = 2\pi \times 10^9 \text{ \AA}^2.$$

Assuming a negative chl-BLM membrane surface charge of $1 \text{ esu}/200 \text{ \AA}^2$, the outer surface of the membrane holds $\sim 3 \times 10^7$ excess negative unit charges. For a membrane capacitance of $5 \times 10^{-9} \text{ F}$, according to the relation $V_m = Q/C_m$ ($1 \text{ esu} = 1.6 \times 10^{-19} \text{ coulombs}$) $V_m = \sim -1 \text{ mV}$.

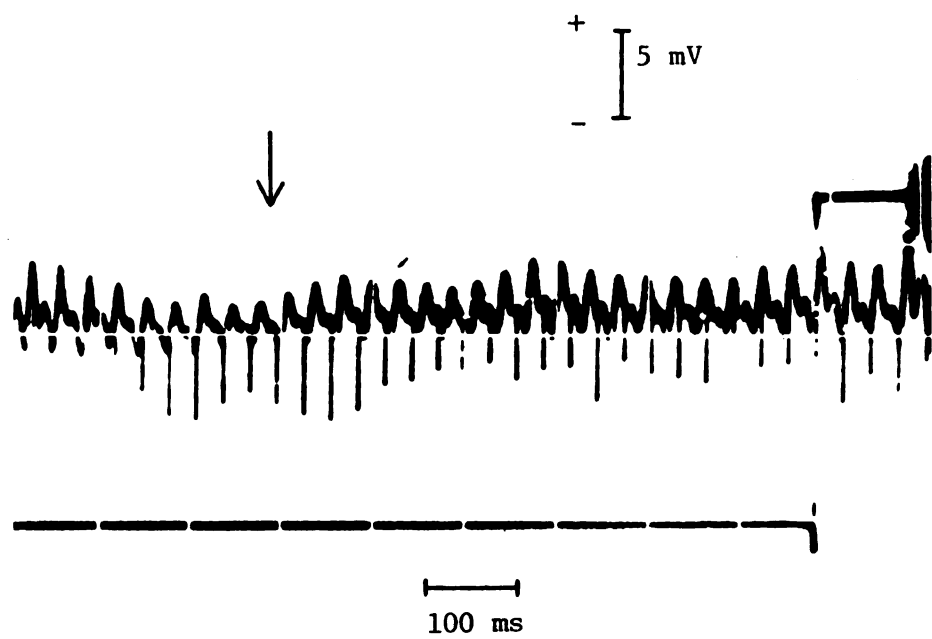
The polarity and magnitude of this result compare favorably with the data given in Figure 20.

Photo-Emf Internal Resistance

Measurements of the equivalent internal resistance of the FeCl_3 induced photo-emf under flash illumination and continuous illumination are useful since this indicates whether the chl-BLM photovoltage device can be loaded, i.e., deliver appreciable currents. As shown in Figures 2 and 12, the initial rapid voltage change requires that a current of at least 10^{-8} amps be delivered in response to microsecond illumination.

A more precise determination of the value of the photobattery internal resistance was made by establishing the value of external

Figure 20. Open circuit BLM potential oscillation synchronous with mechanical vibrations. Superimposed spikes indicate strobe light flashes; arrow denotes moment at which membrane appears maximally distended into the ungrounded electrode chamber.



shunt resistance R_s capable of reducing the absolute magnitude of the Fast Component by half. According to the data recorded in Figure 21, this value of R_s was found to be typically on the order of 5×10^4 ohms. (The electrodes, in series with R_s , presented resistances of approximately this value; therefore this represents a lower limit on possible membrane shunt resistance values.) Notice the extremely short $R_m C_m$ times as expected for Thevenin equivalent resistances reduced to this extent.

Under rapidly repeating flash illumination, an approximation of continuous illumination, a constant photovoltage becomes established across the chl-BLM. As illustrated in Figure 22, the closed circuit current available from the membrane may be determined easily in this case by applying sufficient voltage through shunt resistor R_s to bias the photovoltage to zero. It may be shown that when $V = 0$,

$$E_L/R_L = V_{app}/R_s.$$

In other words, the short-circuited current available from the membrane is simply V_{app}/R_s . This method has been tested experimentally using an ammeter to actually measure these short-circuited currents after expected values of current were calculated as outlined above. The agreement obtained is indicated in Figure 23. These current values correspond to a photobattery internal resistance of $\sim 10^7$ ohms, much greater than the $\sim 5 \times 10^4$ ohms measured as being characteristic of the single flash response photobattery internal resistance.

Concomitantly, membrane FeCl_3 -induced photocurrents fall from a $\sim 10^{-8}$ amp current pulse under brief single flash illumination to approximately 10^{-11} amp under 50 Hz repeated flash illumination.

Figure 21. Effect of low external shunt resistance on the FeCl_3 -induced Fast Component. R_s equals:

1. $2.5 \times 10^5 \Omega$
2. $1.5 \times 10^5 \Omega$
3. $5.0 \times 10^4 \Omega$
4. $1.0 \times 10^8 \Omega$
5. $5.4 \times 10^5 \Omega$
6. $4.0 \times 10^4 \Omega$
7. $3.0 \times 10^4 \Omega$
8. $2.0 \times 10^4 \Omega$

Figure 22. Arrangement used to measure photocurrent output of chl-BLM. At $V = 0$, set by varying V_{app} ,

$$E_L/R_L = V_{app}/R_s$$

Figure 23. Membrane photovoltages (upper trace) returned to zero by application of external voltage biases (lower traces).

Above: $V_{\text{app}}/R_s = 8.8 \times 10^{-11}$ amps; ammeter current measurement, 8.9×10^{-11} amps \pm 5%.

Below: $V_{\text{app}}/R_s = 8.9 \times 10^{-11}$ amps; ammeter current measurement, 8.5×10^{-11} amps \pm 5%.

($R_s = 9.1 \times 10^7 \Omega$)

CHAPTER VII

SUMMARY

Chlorophyll Bimolecular Lipid Membranes are most faithful laboratory reproductions of the essential components of the natural photosynthetic energy transduction device. They successfully meet the cardinal requirements for chlorophyll-dependent photosensitivity and membranous insulating properties to maintain charge separation and insure subsequent chemical reaction rather than energetically wasteful charge recombination. These artificial membranes exhibit photovoltaic responses of two basic types: one represents a reduction potential gradient dependent current that flows in a direction established by the arrangement of redox agents, and the other represents a conductivity increase with kinetic features containing information concerning chlorophyll metastable states in chl-BLM. A study of the latter process offers at least two immediate, direct benefits:

i) Several investigators make extensive use of continuous illumination photoeffects as a tool, but unless the specific molecular excited states responsible for the photoeffect are more fully characterized, interpretations of data can easily be only speculative.

ii) Also, much effort is currently being expended in the study of chlorophyll excited states in vitro (Dutton, Leigh, and Seibert, 1972; Netzel, Rentzepis, and Leigh, 1973) and, provided that λ decay indeed represents chlorophyll triplet decay we have presented a

significant new tool to investigators of chlorophyll photosynthetic excited states as we have incorporated chlorophyll into a membranous matrix akin to the thylakoid membrane of the chloroplast and more highly representative of the in vivo arrangement.

Offering a convenient method for monitoring membranous chlorophyll excited state properties, chlorophyll Bimolecular Lipid Membranes are useful probes into the pathways of photosynthetic energy transduction.

BIBLIOGRAPHY

BIBLIOGRAPHY

- Alamuti, N. and Luger, P. (1970), Biochim. Biophys. Acta, 211, 362.
- Arnon, D.I. (1967), Physiol. Rev., 47, 317.
- Bassham, J.A. and Calvin, M. (1957), "The Path of Carbon in Photosynthesis", Prentice-Hall, Englewood Cliffs, New Jersey, chapter 12.
- Boardman, N.K. (1968), Advances in Enzymology, 30, 1.
- Branton, D. (1969), Annual Review of Plant Physiology, 20, 209.
- Cherry, R.J., Hsu, K. and Chapman, D. (1971), Biochem. Biophys. Res. Commun., 43, No. 2, 351.
- Dutton, P.L., Leigh, J.S. and Seibert, M. (1972), Biochem. Biophys. Res. Commun., 46, No. 2, 406.
- Fujimori, R. and Livingston, R. (1957), Nature, 180, 1036.
- Goldup, A., Ohki, S. and Danielli, J.F. (1970), Recent Progress in Surface Science, 3, 193.
- Gorter, E. and Grendel, F. (1925), J. Med., 41, 439.
- Hesketh, T.R. (1969), Nature, 224, 1026.
- Hong, F.T. and Mauzerall, D. (1972), Nature-New Biol., 240, 154.
- Hong, F.T. and Mauzerall, D. (1972), Biochim. Biophys. Acta, 275, 479.
- Huebner, J.S. and Tien, H.T. (1972), Biochim. Biophys. Acta, 256, 300.
- Huebner, J.S. (1972), J. Memb. Biol., 8, 403.
- Ilani, A. and Berns, D.S. (1972), J. Memb. Biol., 8, 333.
- Kamen, M.D. (1963), "Primary Processes in Photosynthesis", Academic Press, Inc., New York, N.Y.
- Kay, R.E. and Bean, R.C. (1970), Journal of Biological and Medical Physics, 13, 235.
- Kay, R.C. and Chan, H. (1969), Radiation Research, 40, 177.

- Kobamoto, N. and Tien, H.T. (1971), Biochim. Biophys. Acta, 241, 129.
- Kobamoto, N. and Tien, H.T. (1972), Biochim. Biophys. Acta, 266, 56.
- Korneff, T. (1968), "Introduction to Electronics", Academic Press, New York, N.Y.
- Lehninger, A.L. (1970), "Biochemistry", Worth Publishers, Inc., New York, N.Y., p. 460.
- Loxson, F.M. and Tien, H.T. (1972), Chem. Phys. Lipids, 8, 221.
- Livingston, R. and McCartin, P.J. (1963), J. Am. Chem. Soc., 85, 1571.
- Livingston, R. and Pugh, A.C.P. (1960), Nature, 186, 969.
- Mauzerall, D. and Finkelstein, A. (1969), Nature, 224, 690.
- McGlynn, S.P., Azumi, T. and Kinoshita, M. (1969), "The Triplet State", Prentice-Hall, Inc., New Jersey, pp. 40-43.
- Menke, W. (1967), Brookhaven Symp. Biol., 19, 328.
- Moore, W.J. (1963), "Physical Chemistry", Prentice-Hall, Inc., New Jersey, p. 824.
- Mueller, P., Rudin, D.O., Tien, H.T., Wescott, W.C. (1962), Nature, 194, 979.
- Mühlethaler, K. (1966) In: Biochemistry of Chloroplasts. T.W. Goodwin, editor. p. 49. Academic Press Inc., New York.
- Netzel, T.L., Rentzepis, P.M. and Leigh, J. (1973), Science, 182, 238.
- Pant, H.C. and Rosenberg, B. (1971), Photochem. Photobiol., 14, 1.
- Steineman, A., Alamuti, N., Brodmann, W., Marschall, O. and Läger, P. (1971), J. Memb. Biol., 4, 284.
- Steinmann, A., Stark, G. and Läger, P. (1972), J. Memb. Biol., 9, 177.
- Suckling, E.E. (1961), "Bioelectricity", McGraw-Hill Book Company, New York, N.Y.
- Tien, H.T. (1968), Nature, 219, No. 5151, 272.
- Tien, H.T. (1968), J. Phys. Chem., 72, 4512.
- Tien, H.T. and Kobamoto, N. (1969), Nature, 224, 1107.
- Tien, H.T. and Verma, S.P. (1970), Nature, 227, 1232.

- Tien, H.T. (1971), "The Chemistry of Biosurfaces", Hair, M., Ed., Marcel Dekker, Inc., New York, N.Y. pp. 249-255.
- Tien, H.T. (1972), Photochem. Photobiol., 16, 271.
- Tien, H.T. and Howard, R.E. (1972), "Techniques of Surface and Colloid Chemistry and Physics", Marcel Dekker, Inc., New York, N.Y. p. 109.
- Tien, H.T. and Huebner, J.S. (1973), J. Memb. Biol., 11, 57.
- Trissl, H.W. and Luger, P. (1970), Z. Naturforsch., 25, 1059.
- Trissl, H.W. and Luger, P. (1972), Biochim. Biophys. Acta, 282, 40.
- Ullrich, H. and Kuhn, H. (1969), Z. Naturforschg., 24b, 1342.
- Ullrich, H. and Kuhn, H. (1972), Biochim. Biophys. Acta, 266, 584.
- Van, N.T. and Tien, H.T. (1970), J. Phys. Chem., 74, No. 20, 3559.
- Verma, S.P. (1971), Biophysik, 7, 228.
- Verma, S.P. (1971), Indian Journal of Chemistry, 9, No. 9, 1012.
- Vernon, L.P. and Seely, G.R. (1966), "The Chlorophylls", Academic Press, New York, N.Y.

MICHIGAN STATE UNIVERSITY LIBRARIES



3 1293 03169 6580